[Papers in Palaeontology, Vol. 12, Part 2, 2026, e70069]

A new taxon of saurischian dinosaur from the *Coelophysis* Quarry of New Mexico, USA (Triassic: latest Norian or Rhaetian) highlights herrerasaurian diversity in the latest Triassic

by SIMBA SRIVASTAVA* *and* STERLING J. NESBITT

Department of Geosciences, Virginia Tech, Blacksburg, Virginia 24061, USA; simba@vt.edu, sjn2104@vt.edu
*Corresponding author

Typescript received 28 February 2025; accepted in revised form 19 December 2025

Abstract: The most complete record of the earliest dinosaur lineages is from the Carnian from the higher latitudes of Pangea (e.g. present-day Brazil, Argentina), but dinosaurian assemblages from the upper stages of the Upper Triassic are better known from the low latitudes of Pangea (present day southwestern USA). How early carnivorous dinosaurian diversity matches or mismatches at various latitudes remains to be documented because of uncertainty around the spatio-temporal ranges and phylogenetic relationships of early dinosaur lineages. We examine low-latitude diversity patterns through the lens of the saurischian dinosaur *Tawa hallae* and close relatives, including a new species, *Ptychotherates bucculentus* gen. et sp. nov. The new taxon is known from an incomplete but well-preserved skull (CM 31368) from the uppermost Triassic *Coelophysis* Quarry in northern New Mexico. The new taxon clearly shares synapomorphies with *Tawa hallae*, such as distinctive fossae on the quadrate and otoccipital and a dorsoventrally tall and laterally flat jugal. However, the new taxon is distinguishable from all other coeval ornithodirans by a combination of many character states, including the proportionally dorsoventrally deepest jugal known for any Triassic-aged dinosaur. Higher-palaeolatitude ecosystems across Pangea show a complete turnover of carnivorous dinosaurs by neotheropods in the Norian and Rhaetian, but the '*Chindesaurus–Tawa*' clade (Morphoraptora clade nov.) coexisted with neotheropods possibly until the End-Triassic Extinction Event. This suggests a low-latitude 'museum' where early-diverging lineages survived much longer than at higher latitudes, and that the End-Triassic Extinction Event affected dinosaur diversity more than previously hypothesized.

Key words: biogeography, Saurischia, extinction, skull, phylogenetics, clade longevity.

DINOSAURS originated in the Carnian Stage, the earliest part of the Late Triassic, and subsequently diverged into three Jurassic-surviving lineages: Ornithischia, Theropoda and Sauropodomorpha (Rogers *et al.* 1993; Sereno 1997; Brusatte *et al.* 2010; Langer *et al.* 2010, 2018; Martinez *et al.* 2011; Marsicano *et al.* 2016). Nearly all of the earliest dinosaur remains come from the high-latitude southern part of Pangea (i.e. present-day Brazil, Argentina, Zimbabwe, India; Sereno *et al.* 1993; Brusatte *et al.* 2010; Langer *et al.* 2010; Novas *et al.* 2010; Ezcurra 2012; Novas *et al.* 2021; Griffin *et al.* 2022) whereas the lower latitudes (i.e. Upper Triassic deposits of the American Southwest, Morocco) have few, if any, diagnostic dinosaur remains from the equivalent age (Irmis *et al.* 2011; Ramezani *et al.* 2011; Ezcurra 2012; Fitch *et al.* 2020; Marsh & Parker 2020; Lovelace *et al.* 2025; Mujal *et al.* 2025).

Few fossiliferous sites worldwide preserve diagnostic dinosaurian fossils from the uppermost stage of the Triassic (i.e. Rhaetian), hampering our tracing of the evolution of both dinosaurian assemblages and lineages throughout this important time in dinosaurian evolution. The few Rhaetian-aged exposures, such as in India (Novas *et al.* 2010), USA (Nesbitt *et al.* 2009; Marsh & Parker 2020), Argentina and Brazil (Novas *et al.* 2021), and central (Mujal *et al.* 2025) and western Europe (Weeks *et al.* 2025) hint at a temporally distinct, but globally consistent dinosaur assemblage composition: Rhaetian fossils only of sauropodomorph and neotheropod dinosaurs have been uncovered, with the exception of the phylogenetically problematic saurischian *Daemonosaurus chauliodus* from southwestern USA (Nesbitt & Sues 2021). Older Triassic exposures from the Carnian and Norian stages of the Late Triassic feature other carnivorous clades

doi: 10.1002/spp2.70069

of saurischians, such as herrerasaurians, but no clearly identifiable members of these lineages are represented towards the end of the Triassic anywhere in Pangea.

To examine the dinosaur assemblages at low latitudes, we focus on the Late Triassic dinosaurian assemblages of southwestern USA, namely those comprising the Chinle Formation and Dockum Group. Compared with other early dinosaur assemblages, these are aberrant in that they preserve multiple carnivorous dinosaur lineages but no sauropodomorphs (Irmis *et al.* 2007; Marsh & Parker 2020; but see Lovelace *et al.* 2025), which is attributed to the unique environmental conditions faced in the low-palaeolatitude arid belts of Pangea (Kent & Irving 2010; Whiteside *et al.* 2015). Morphoraptora clade nov., a clade of carnivorous saurischians best represented by the saurischians *Tawa hallae* and *Chindesaurus bryansmalli*, as well as fragmentary postcranial remains that have been loosely diagnosed through apomorphy-based identification (Stocker 2013; Marsh *et al.* 2019; Marsh & Parker 2020), features a combination of herrerasaurian and neotheropod traits, indicating a phylogenetically critical point to study in the early radiation of Dinosauria. The clade occurs stratigraphically alongside neotheropods such as *Lepidus praecisio* (Nesbitt & Ezcurra 2015) in parts of the Chinle Formation and Dockum Group.

The stratigraphically youngest rocks of the Chinle Formation, however, have yet to yield these *Tawa*-like forms. The Rhaetian-aged (possibly latest Norian) *Coelophysis* Quarry at Ghost Ranch, northern New Mexico, was deposited as the mass burial of thousands of individuals of a single, coeval fauna (Schwartz & Gillette 1994; Rinehart *et al.* 2009), and the most common taxon by far is the eponymous neotheropod dinosaur *Coelophysis bauri*. The saurischian *Daemonosaurus chauliodus* was described from *Coelophysis* Quarry material by Sues *et al.* (2011) as the second dinosaur from the assemblage, but only from a single crushed skull and a few cervical vertebrae. However, its distinct morphology and proportions are not similar to other early-diverging dinosaurs, and its relationships are not well resolved (Nesbitt & Sues 2021).

Here, we describe the third dinosaur from the *Coelophysis* Quarry based on a partial skull of a *Tawa*-like dinosaur, *Ptychotherates bucculentus* (CM 31368, Figs 1–3). This new taxon extends the stratigraphic range of *Tawa*-like dinosaurs towards the end of the Triassic, and it expands the diversity of the dinosaurian assemblage of low-latitude Pangea at that time, as well as the morphological disparity among Triassic dinosaurs.

METHOD

The holotype underwent computed tomography (CT) scanning at the Shared Materials Instrumentation Facility (SMiF) at Duke University using a Nikon XTH 225 ST. CT scans were rendered and segmented using Materialise Mimics v20. Matrix and bone would frequently overlap in density, necessitating manual segmentation either slice by slice or by computer interpolation of up to five intermediary slices at a time. This overlap was often too great and precluded any reliable segmentation for many bones that are obscured or close to other bones, such as the tooth roots and parts of the braincase. We prioritized segmentation of the parts of the skull that preserve overlapping anatomy with the comparison taxa, and which can be scored for characters in the selected phylogenetic datasets. The braincase was not segmented and will be described at a later date. The CT dataset is available in MorphoSource (Srivastava & Nesbitt 2025).

Hypotheses of evolutionary relationships for *Ptychotherates bucculentus* were tested in two character matrices that broadly sample Triassic-aged ornithodirans and their relatives and which have been continuously revised since their first publication. One was derived from the latest iteration of the matrix erected by Baron *et al.* (2017a) and implemented with additional taxa, characters, and corrections last published by Griffin *et al.* (2022). The other was derived from a dataset first published by Nesbitt *et al.* (2009) and implemented with additional taxa, characters, and corrections last published by Ezcurra *et al.* (2023).

The Baron *et al.* (2017a) analysis was erected to test the relationships among a sample of early dinosaurs with a focus on early-diverging clades (we defer to the scorings published by Langer *et al.* 2017); this provided a wide-sampling assessment of the relationships of *Ptychotherates bucculentus* to a broad array of ornithodirans. We scored *Ptychotherates bucculentus* in this dataset, added two characters (390 and 391) and modified one character (382), so that this dataset now has 83 taxa and 459 characters (24, 35, 39, 60, 68, 71, 117, 145, 167, 169, 174, 180, 197, 199, 206, 214, 215, 222, 251, 269, 272, 286, 289, 303, 305, 307, 313, 322, 333, 334, 338, 353, 360, 376, 378, 387, 393, 442, 446 ordered). The pre-existing scores for a few other taxa were modified (Appendix S1). *Agnosphitys cromhallensis*, *Nyasasaurus parringtoni* and *Saltopus elginensis* were removed from all analyses on the justification given by Griffin *et al.* (2022) regarding their preservation and validity.

The second dataset, originally from Nesbitt *et al.* (2009), now focuses more on early-diverging neotheropods (Ezcurra *et al.* 2023), and serves as another test of the relationships of *Ptychotherates bucculentus* to other carnivorous dinosaurs. This was also the dataset used by Marsh *et al.* (2019) to further test the relationships of *Chindesaurus bryansmalli*, resulting in a close relationship between *Tawa hallae* and *Chindesaurus bryansmalli*. After scoring *Ptychotherates bucculentus*, adding the same

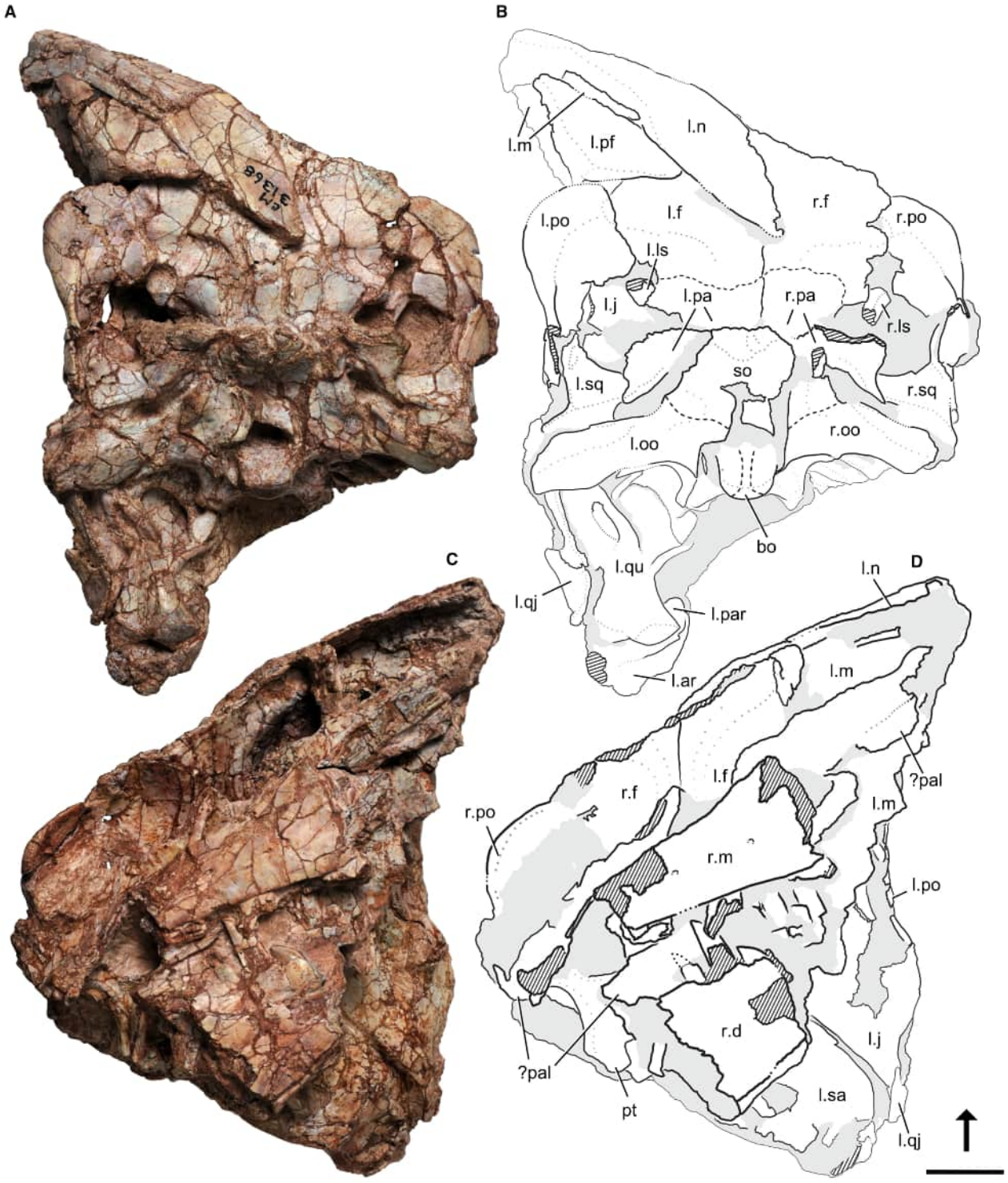

FIG. 1. The holotype skull of *Ptychotherates bucculentus* (CM 31368). A–B, photograph (A) and interpretative line drawing (B) of dorsal view of skull roof. C–D, photograph (C) and interpretative line drawing (D) of right lateral view of right dentary and maxilla. *Abbreviations*: l., left; r., right; ar, articular; bo, basioccipital; d, dentary; f, frontal; j, jugal; ls, laterosphenoid; m, maxilla; n, nasal; oo, otoccipital; pa, parietal; pf, prefrontal; po, postorbital; pt, pterygoid; par, prearticular; qu, quadrate; qj, quadratojugal; sa, surangular; so, supraoccipital; sq, squamosal; ?pal, possible palatal elements. Arrow indicates anterior direction relative to the braincase. Stripes indicate broken surfaces, dashed lines show hypothesized element contacts, and light grey represents matrix. Scale bar represents 2 cm.

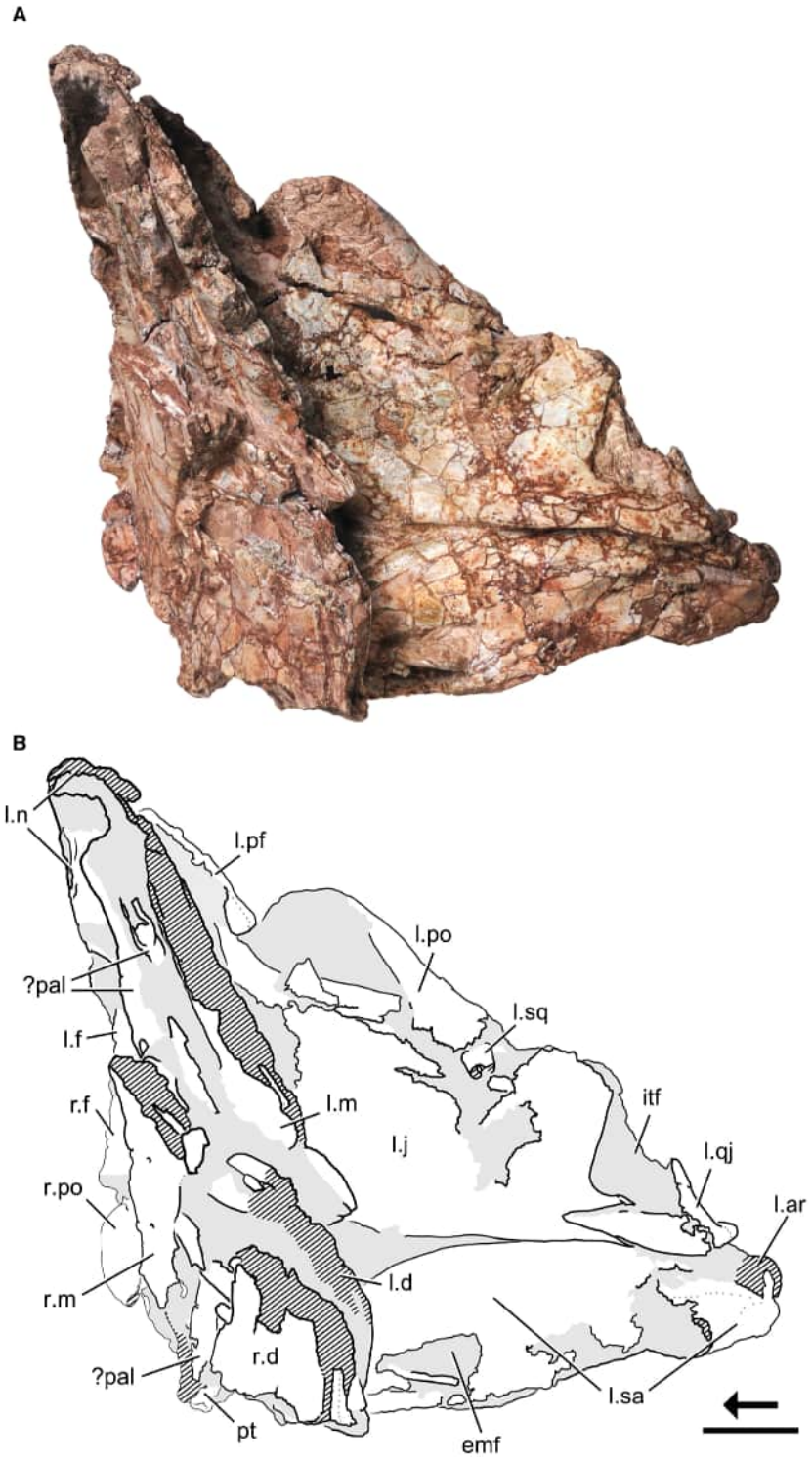

FIG. 2. The holotype skull of *Ptychotherates bucculentus* (CM 31368) in left lateral view relative to the left jugal and surangular: A, photograph; B, interpretive line drawing. *Abbreviations*: l., left; r., right; ar, articular; d, dentary; emf, external mandibular fenestra; f, frontal; itf, infratemporal fenestra; j, jugal; m, maxilla; n, nasal; pf, prefrontal; po, postorbital; pt, pterygoid; qj, quadratojugal; sa, surangular; sq, squamosal; ?pal, possible palatal elements. Arrow indicates anterior direction relative to the braincase. Stripes indicate broken surfaces and light grey represents matrix. Scale bar represents 2 cm.

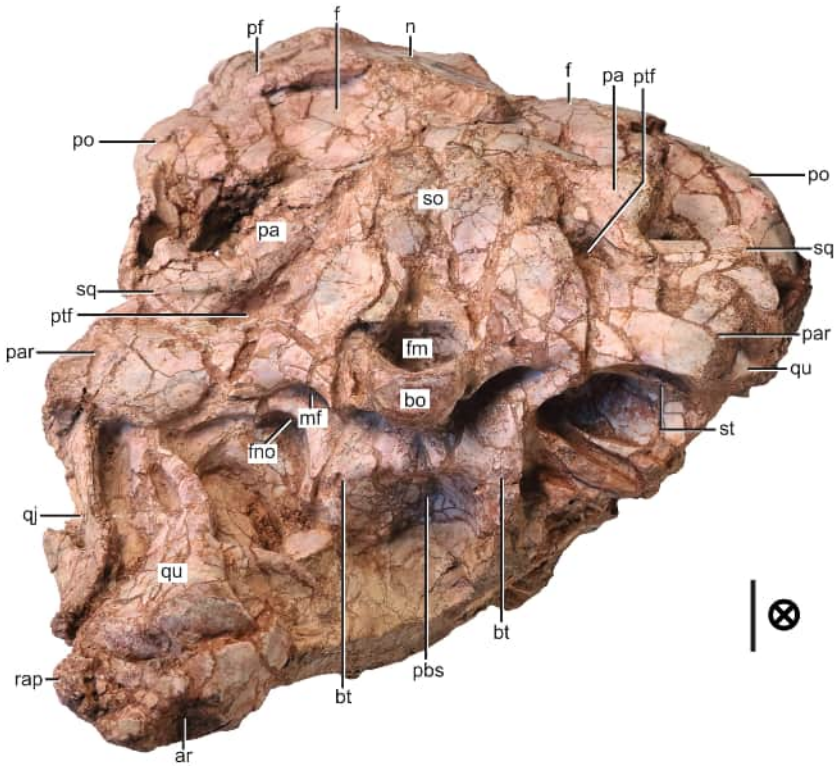

FIG. 3. The posterior portion of the skull *Ptychotherates bucculentus* (CM 31368) in posterior view. *Abbreviations*: ar, articular bo, basioccipital; bt, basituber; f, frontal; fm, foramen magnum; fno, fenestra ovalis; pa, parietal; par, paroccipital process of the otoccipital; mf, metotic foramen; n, nasal; pbs, parabasisphenoid; pf, prefrontal; po, postorbital; ptf, posttemporal fenestra; qj, quadratojugal; qu, quadrate; rap, retroarticular process; so, supraoccipital; sq, squamosal; st, stapes. Crossed circle indicates posterior direction out of page. Scale bar represents 1 cm.

characters as for the first dataset (458 and 459), and modifying one character in a similar manner to the first dataset (69), this dataset now has 64 taxa and 391 characters (9, 18, 30, 67, 128, 129, 174, 184, 197, 207, 213, 219, 231, 236, 248, 253, 254, 273, 329, 343, 345, 347, 349, 354, 366, 371, 374, 377–379, 383, 384 ordered). In addition to scoring *Ptychotherates bucculentus*, the pre-existing scores for a few other taxa were modified after revaluation (Appendix S1). *Nhandumirim waldsangae* was also removed from all analyses due to uncertainty about its taxonomic status, as were the highly incomplete holotypes of *Lepidus praecisio* and *Powellvenator podocitus*, although combined score sets from multiple specimens of the latter two taxa were included in the matrices.

Both datasets were edited in Mesquite v3.81, and analyses were performed in TNT v1.6 (Goloboff & Morales 2023). Analyses began by allotting 78 megabytes of RAM to the tree-building program (command line 'mxram 78'), importing a character matrix as a .tnt file, then setting the memory space to 100 000 trees. We implemented 10 000 replications of tree bisection–reconnection, saving 10 trees per replication and collapsing zero-length branches ('collapse trees after the search'), then implemented a second round of tree bisection–reconnection using the trees from the first round as seeds, and constructed strict consensus trees after removing suboptimal trees (command line 'best'). Bremer supports were also calculated in TNT by producing trees up to 10 steps suboptimal to the best trees through bisection–reconnection. Bootstrap resampling GC (group contradicted) frequencies were yielded from standard bootstrap resampling with 1000 replicates, with 10 replications of tree bisection–reconnection per replicate.

Institutional abbreviations. AMNH, American Museum of Natural History, New York, NY, USA; CAPPA/UFSM, Centro de Apoio à Pesquisa Paleontologica da Quarta Colonia da Universidade Federal de Santa Maria, São João do Polêsine, RS, Brazil; CM, Carnegie Museum of Natural History, Pittsburgh, PA, USA; DMNH, Dallas Museum of Natural History, Dallas, TX, USA; GR, Ruth Hall Museum of Paleontology, Ghost Ranch, Abiquiu, NM, USA; MCP, Museu de Ciências e Tecnologia da Pontifícia Universidade Católica do Rio Grande do Sul, Porto Alegre, Brazil; MNA, Museum of Northern Arizona, Flagstaff, AZ, USA; NCSM, North Carolina Museum of Natural Sciences, Raleigh, NC, USA; NHMZ, Natural History Museum of Zimbabwe, Bulawayo, Zimbabwe; NMS.G, National Museums Scotland,

Edinburgh, UK; NMT, National Museum of Tanzania, Dar es Salaam, Tanzania; PEFO, Petrified Forest National Park, AZ, USA; PULR, Paleontologia, Universidad Nacional de La Rioja, La Rioja, Argentina; PVSJ, Museo de Ciencias Naturales, Universidad Nacional de San Juan, San Juan, Argentina; SMF, Saurier-museum Frick, Canton Aargau, Switzerland; SMNS, Staatliches Museum für Naturkunde Stuttgart, Stuttgart, Germany; TTU, Texas Tech University Museum, Lubbock, TX, USA; UCMP, University of California Museum of Paleontology, Berkeley, CA, USA; ULBRA, Museu de Ciências Naturais, Universidade Luterana do Brasil, Canoas, RS, Brazil; USNM, National Museum of Natural History (formerly United States National Museum), Smithsonian Institution, Washington DC, USA; ZPAL, Institute of Paleobiology of the Polish Academy of Sciences, Warsaw, Poland.

SYSTEMATIC PALAEONTOLOGY

DINOSAURIA Owen 1842 *sensu* Langer *et al.* 2020
SAURISCHIA Seeley 1888 *sensu* Gauthier *et al.* 2020
Clade MORPHORAPTORA nov.

Derivation of name. *Morphe* from the Greek for 'form, shape' and *raptor* from the Latin for 'robber', describing the morphological convergence between members of this clade and Theropoda, as if this clade is 'stealing' morphology. 'Morphoraptor' loosely translates to 'bodysnatcher', in honour of the 2007 song by Radiohead in the album *In Rainbows*, which author SS listened to hundreds of times while preparing this manuscript.

Definition. The most inclusive clade containing *Tawa hallae* Nesbitt *et al.* 2009, but not *Herrerasaurus ischigualastensis* Reig 1963, *Passer domesticus* Linnaeus 1758, *Saltasaurus loricatus* Bonaparte & Powell 1980, *Triceratops horridus* Marsh 1889, *Silesaurus opolensis* Dzik 2003 or *Pterodactylus antiquus* Sömmerring 1812.

Diagnosis. Morphoraptorans are diagnosed by: fine serrations on the teeth (4–5 per 1 mm in the maxilla, 5–6 per 1 mm in the dentary) with pointed apices; ventral recess of the parabasisphenoid wide with a centrally located foramen.

Postcranially, *Tawa hallae* (GR 241) and *Chindesaurus bryansmalli* (PEFO 10395) share a rimmed depression on the anterior part of the cervical centra. We tentatively suggest that this diagnoses Morphoraptora because it is not clear whether *Daemonosaurus chauliodus* has the exact same condition, or whether this clade is more closely related to theropod dinosaurs than to other major dinosaur lineages (i.e. Ornithischia, Sauropodomorpha, Herrerasauridae), in which case this feature would represent a plesiomorphy and not an apomorphy.

Remarks. We designate Morphoraptora as a formal clade name to replace the informal '*Chindesaurus-Tawa*' clade used in previous publications (e.g. Marsh *et al.* 2019; Ezcurra *et al.* 2025). The core of this clade contains *Ptychotherates bucculentus*, *Tawa hallae* and *Chindesaurus bryansmalli*. In this study, our phylogenetic analyses consistently recovered *Daemonosaurus chauliodus* as a closer relative to *Tawa hallae*, *Chindesaurus bryansmalli* and *Ptychotherates bucculentus*. Notably, *Daemonosaurus chauliodus* is never recovered as more closely related to *Tawa hallae* than are *Chindesaurus bryansmalli* or *Ptychotherates bucculentus*.

Genus †*Ptychotherates* nov.

LSID. https://zoobank.org/NomenclaturalActs/c96ab9e2-59ee-4758-bb95-ec4253831cb9

Derivation of name. *Ptycho* from the Greek for 'fold' because of the numerous and challenging axes of reorientation on elements of the holotype. *Therates* from the Greek for 'hunter', for the carnivorous habits inferred from its teeth.

Type species. *Ptychotherates bucculentus* (by monotypy).

Diagnosis. As for type and only known species.

†*Ptychotherates bucculentus* sp. nov. Figures 1–3

LSID. https://zoobank.org/NomenclaturalActs/f270573f-6a0b-4680-ab56-11eecbe2f5df

Derivation of name. The species epithet is Latin for 'with full cheeks' in reference to the exceptionally tall jugal.

Holotype. The only material ascribed herein to *Ptychotherates bucculentus* (CM 31368) is a mostly complete and partially articulated skull with a complete braincase and much of the skull roof, as well as some palatal and hemimandibular elements. Preserved skull elements include: partial left and right maxillae; incomplete left nasal; complete left prefrontal; incomplete left and right frontals; complete left and right parietals; nearly complete left and right postorbitals; nearly complete left and right squamosals; mostly complete left jugal; mostly complete left quadratojugal; mostly complete left quadrate and parts of the right quadrate; fragmentary palatine; fragmentary pterygoid; complete braincase (complete supraoccipital, basioccipital otoccipitals, parabasisphenoid, laterosphenoids); mostly complete left surangular with articulated articular and partial prearticular; and partial dentaries.

Diagnosis. *Ptychotherates bucculentus* bears the following combination of character states (local autapomorphies indicated with *): supratemporal fossa present on posterior portion of the frontal and dorsal surface of the parietal; tapering dorsal process of the maxilla; maxilla lacking antorbital fossa on its posterior portion ventral to the antorbital fenestra; prefrontal symmetrical in lateral view*; jugal body proportionally dorsoventrally deep* (i.e. more than three times as deep as the jugal posterior process, deeper than the length of postorbital ventral process, and more than half the height of the quadrate main body; Table 1);

TABLE 1. Comparison of cranial measurements (in mm) between Triassic dinosaurs.

Taxon	Jugal height*	Jugal posterior (= quadratojugal) process height†	Quadrate height	Postorbital ventral (= jugal) process length
Ptychotherates bucculentus	29	7	42	26
Tawa hallae (GR 241, pers. obs.)	13	–	34	22
Daemonosaurus chauliodus (CM 76821, pers. obs. of cast)	11	7	>46	33
Pampadromaeus barberenai (ULBRA-PVT-016, Langer *et al.* 2019 figs 8, 9)	2.5	3.2	>27	23
Zupaysaurus rougieri (PULR-V 076, Ezcurra 2007 fig. 3)	16	16	110	88
Plateosaurus (AMNH-FARB 6810, pers. obs. of resin print)	13	10	86	54
Herrerasaurus ischigualastensis (PVSJ 407, pers. obs. of cast)	21	10	54	53

*Below dorsoventrally tallest point of orbit.
†Orthogonal to main axis of process.

laterally extensive ventral process (= crista interfenestralis) of the otoccipital; ventral process of squamosal anteroposteriorly wide with a lateral fossa on the posterior part; retroarticular process upturned immediately posterior to glenoid; anterolateral portion of postorbital dorsally overhanging orbit; postorbital dorsolaterally overlapping the squamosal; posttemporal fenestra as wide as foramen magnum; nasal and frontals flat dorsally; serrated and recurved teeth with fine serrations (4–5 per 1 mm in the maxilla, 5–6 per 1 mm in the dentary) with pointed apices of the serrations.

Differs from all other archosaurs other than *Tawa hallae* (GR 241) in the following character states: jugal laterally flat and proportionally tall ventral to the orbit (i.e. deeper than half the length of postorbital ventral process and more than one-third the height of the quadrate main body, Table 1); deep fossa on the posterior edge of the quadrate in posterior view; well-defined fossa on the dorsal surface of the paroccipital process of the braincase; fine serrations on the teeth (4–5 per 1 mm in the maxilla, 5–6 per 1 mm in the dentary) with pointed apices; ventral recess of the parabasisphenoid wide with a centrally located foramen.

Differs from *Tawa hallae* (GR 241) in the following character states: proportionally deeper jugal (i.e. deeper than the length of postorbital ventral process and more than half the height of the quadrate main body; Table 1); labial surface of dentary and maxillary tooth crowns smooth without ridges or grooves; proportionally longer anterior portion of the prefrontal so that the element is symmetrical in lateral view; proportionally shorter ventral process of the prefrontal; more laterally pronounced surangular ridge; surangular with a dorsally arched dorsal margin, as seen in lateral view; possibly deeper dentary; articular groove demarcation on ventral process of the postorbital rounded in transverse cross-section; dorsal articular head of the quadrate more circular in transverse outline.

Ptychotherates bucculentus cannot strictly be distinguished from *Chindesaurus bryansmalli* because the holotypes lack any anatomical overlap. Although it will always be difficult to demonstrate that they are different taxa based on anatomy and they are likely to be closely related, they show distinct stratigraphic separation: specimens referred to *Chindesaurus bryansmalli* are older than 209.926 ± 0.072 Ma (Ramezani *et al.* 2011) in the Revueltian holochronozone (Marsh *et al.* 2019) of Petrified Forest National Park, Arizona, whereas *Ptychotherates bucculentus* is younger than 211.9 ± 0.7 Ma (Irmis *et al.* 2007, 2011), possibly up to 5–9 myr younger, and is from the Apachean holochronozone (Lucas 1998; see Locality and age).

Ptychotherates bucculentus can be easily differentiated from its contemporary dinosaurs found in the same locality (i.e. *Coelophysis* Quarry). *Ptychotherates bucculentus* differs from *Coelophysis bauri* in many aspects of the skull of the former, including (but not a comprehensive list, see description): postorbital with a broad contact with the frontal; jugal much taller ventral to the orbit and lacking a lateral ridge; quadrate with deep fossa on the posterior edge; maxilla lacking the broad lateral antorbital fossa present in *Coelophysis bauri*; proportionally larger posttemporal fenestra. *Ptychotherates bucculentus* differs from *Daemonosaurus chauliodus* in that the skull of *Ptychotherates bucculentus* possesses both a proportionally deeper jugal that lacks a lateral ridge and a proportionally much smaller prefrontal (see description for other differences).

Locality & age. CM 31368 was prepared out of excavation block C-3-82 (i.e. Carnegie Museum block 3 from 1982) from the *Coelophysis* Quarry, Ghost Ranch, northern New Mexico, USA (Fig. 4A, B). This block was collected by the Carnegie Museum of Natural History, and the relative location of block C-3-82 relative to the other removed fossil blocks is available in figures such as Colbert (1989, fig. 6) and Rinehart *et al.* (2009, fig. 4). However, we do not know exactly where the skull came from in block C-3-82.

Multiple independent lines of evidence suggest that the *Coelophysis* Quarry, located in the informal 'siltstone member' of the Chinle Formation of the Chama Basin, is of latest Triassic age, possibly Rhaetian (Fig. 4C). The locality lies 65 m stratigraphically above, and is lithologically distinct from, Hayden Quarry 2 in the Petrified Forest Member, which has been isotopically dated to *c.* 211.9 ± 0.7 Ma to the upper Norian Stage (Irmis *et al.* 2007, 2011). A more involved lithostratigraphic argument for an end-Triassic age is presented by Lucas *et al.* (2005) and further supported by Zeigler *et al.* (2008), and although the distant Wingate and Nugget Sandstones bear Triassic rock overlying the Chinle Formation elsewhere, the 'siltstone member' may overlap chronologically with them. Biostratigraphically, the

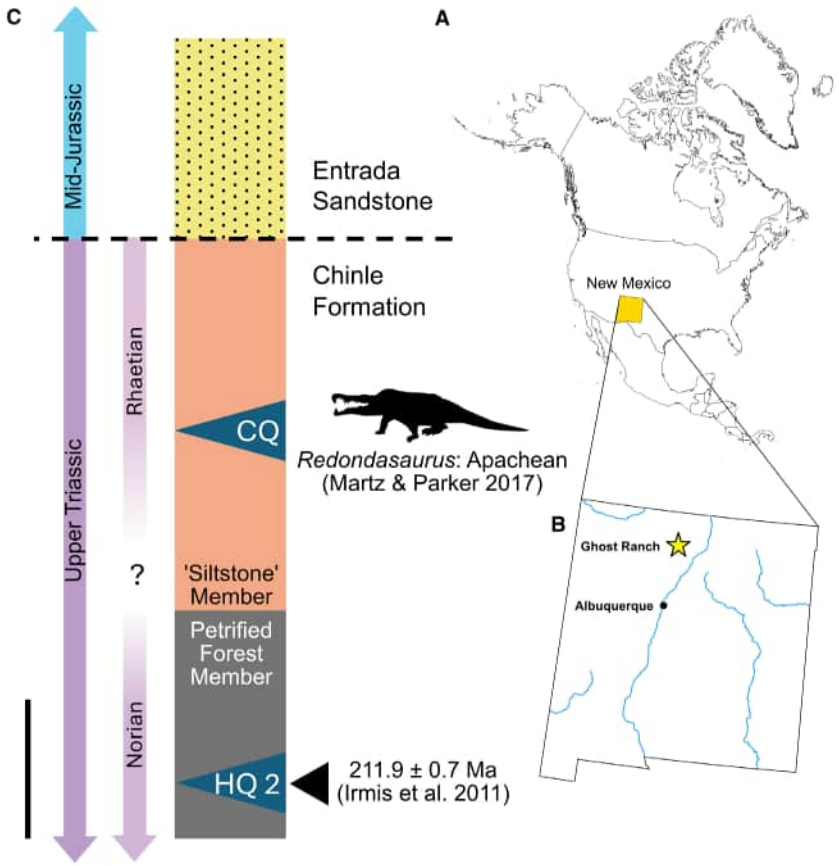

FIG. 4. Summarized stratigraphic and locality data for the holotype of *Ptychotherates bucculentus* (CM 31368). A, a map of North America highlighting New Mexico. B, a map of New Mexico, USA with a yellow star indicating the general location of Ghost Ranch. C, a simplified stratigraphic section of Ghost Ranch; the black triangle indicates a radioisotope-derived date, the black star indicates the source stratum for CM 31368, and the horizontal dashed line represents an unconformity. *Abbreviations*: CQ, *Coelophysis* Quarry; HQ 2, Hayden Quarry 2. Scale bar represents 25 m (C). Phytosaur silhouette by Robert Gay (CC BY-SA 3.0).

presence of the deeply nested phytosaur genus *Redondasaurus* from the *Coelophysis* Quarry is shared with the Owl Rock Member of the Chinle Formation, which is radioisotopically dated to the Rhaetian Stage (Ramezani *et al.* 2011; Martz & Parker 2017, but see Kent *et al.* 2019 for a magnetochronological argument for a slightly older age of the Owl Rock Member). An eastern North American magnetochron close to the Triassic–Jurassic boundary may correlate to one immediately stratigraphically above the *Coelophysis* Quarry, also supportive of an end-Triassic age (Zeigler & Geissman 2011). No absolute age is reported from the 'siltstone member' or the *Coelophysis* Quarry itself.

Ontogenetic assessment. CM 31368 lacks any appendicular elements for an osteohistological analysis of ontogenetic age. There is also a lack of cranial ontogenetic series for closely related taxa, therefore we refrain from any certain ontogenetic diagnosis. The exoccipital component of the otoccipitals is fully ossified with the basioccipital to form a rounded occipital condyle, but this feature alone is not a reliable indicator of ontogenetic age (Griffin *et al.* 2021).

Remarks. The skull is most complete around the braincase, articulated with the skull roof and closely associated with other cranial bones. The front of the skull has collapsed and flattened to align in parallel underneath or anterior to the braincase (Fig. 1). The snout and palate have generally been upturned, rotated counterclockwise in anterior view and shifted posteriorly. Consequently, the maxillae and dentaries lie in oblique right ventrolateral view when the left jugal and surangular are in lateral view (Fig. 2). The left nasal and prefrontal are inclined *c.* 40° anterolaterally from the midline in dorsal view. The jugal and surangular–articular were upturned and rotated to the right; those elements, the quadrate and skull roof were dorsally compressed. This complexity of three-dimensional disarticulation is distinct from other *Coelophysis* Quarry sauropsid skulls, such as the simple dorsoventral compression of a specimen of *Hesperosuchus agilis* (CM 29894, Clark *et al.* 2001), the mediolaterally compressed holotype of *Daemonosaurus chauliodus* (CM 76821, Sues *et al.* 2011) and the typically unilaterally compressed skulls of *Coelophysis bauri*

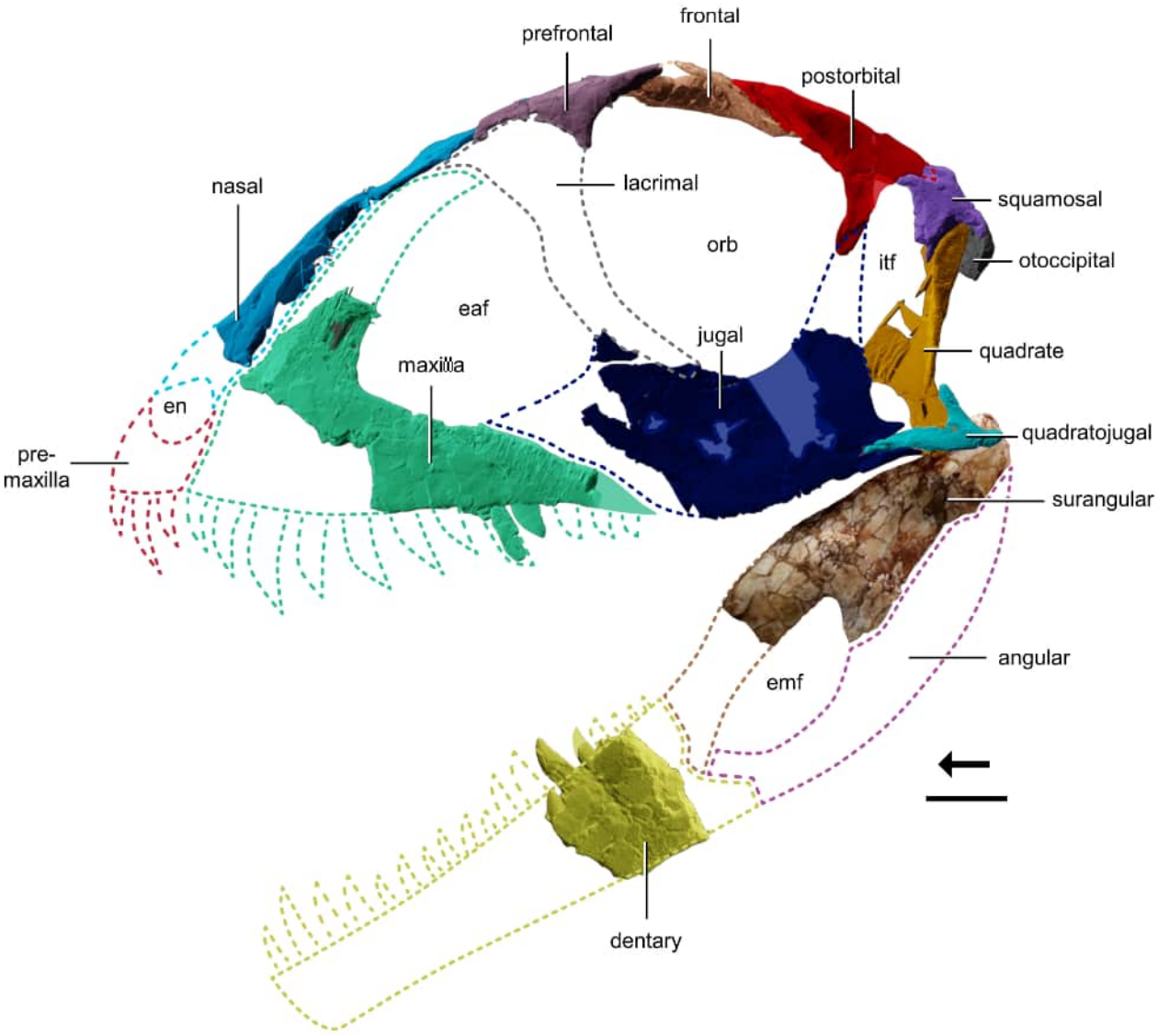

FIG. 5. Digital reconstruction of the skull of *Ptychotherates bucculentus* (CM 31368) in left lateral view. Dashed lines indicate extrapolation and the coloured infill indicates known bone presence. *Abbreviations*: eaf, external antorbital fenestra; en, external naris; emf, external mandibular fenestra; itf, infratemporal fenestra; orb, orbit. Arrow indicates anterior direction. Scale bar represents 2 cm.

(e.g. AMNH 7227 and AMNH 7228). We deduce that the skull had been partially disarticulated prior to fossilization and may have been trampled.

DESCRIPTION

Anatomical orientation & terms

We use 'Romerian' terms as per Wilson (2006) (e.g. 'anterior' instead of 'rostral' and 'posterior' instead of 'caudal'). For teeth, we use the terminology assembled by Hendrickx *et al.* (2015).

Skull reconstruction

In reconstructing the skull of *Ptychotherates bucculentus* (CM 31368), we started with the skull elements that remain in articulation, used other early-diverging dinosaurs and closely related taxa as a guide (e.g. *Tawa hallae*, *Herrerasaurus ischigualastensis*), and used digital separation of elements using CT scans (Fig. 5).

The jugal and quadratojugal were preserved in articulation with each other, as were the quadrate, squamosal, postorbital, frontal and braincase with one another. The prefrontal was aligned with the crista cranii of the ventral surface of the frontal and the curvature of the frontal in

lateral view. Due to inferred plastic deformation in the anterior section of the nasal, and a crack in the posterior section, the nasal was rectified using the 'pose' tool in Blender sculpt mode and by aligning the halves on either side of the crack. The nasal was then oriented with the medial edge as the midline and the posterolateral edge in contact with the anteromedial edge of the prefrontal. The maxilla was positioned primarily using the more complete left maxilla, with the right maxilla aligned and superimposed to show the fraction of the tooth row that it preserves more than the left maxilla. The maxilla was oriented so that the ventral edge was continuous with the ventral edge of the jugal and the anterodorsal edge was aligned with the ventrolateral edge of the nasal for the maxilla–nasal contact. The quadratojugal was also altered at a mediolaterally oriented crack that artificially narrowed the interior angle between the dorsal and anterior processes, and the postorbital is a composite of sections of both counterparts. The dentary was arranged so that its preserved teeth were mesiodistally positioned in occlusion with the preserved maxillary teeth. The figured postdentary bones were incorporated from a surface scan rather than a mesh.

The resulting skull is *c.* 22 cm long (anteroposteriorly) and 10 cm deep (dorsoventrally) at its deepest point at the anteroposterior middle of the top of the orbit, although shearing and anteroposterior compression of the temporal and braincase regions may artificially be doming the top of the skull. Even so, the large and dorsoventrally deep jugal and maxilla of *Ptychotherates bucculentus* result in a relatively taller skull than coeval *Coelophysis bauri* and the close relative *Tawa hallae* (GR 241). We reconstruct the anterior portion of the skull as tapering anteroventrally in lateral view, primarily in controlling for orbit size and shape through the orientation of the prefrontal. This contrasts with the more rectangular snouts of herrerasaurids such as *Gnathovorax cabreirai* (CAPPA/UFSM 0009) or *Herrerasaurus ischigualastensis* (PVSJ 407). The ventral edge of the orbit was set substantially higher than the base of the antorbital fenestra in *Ptychotherates bucculentus*, similarly to *Tawa hallae* (GR 241) but unlike any other Triassic dinosauromorph, for which they are about in the same horizontal plane (e.g. *Daemonosaurus chauliodus*, CM 76821; *Eoraptor lunensis*, PVSJ 512).

Maxilla

Both maxillae are laterally exposed and preserve a segment of the posterior process (=jugal ramus, 'pp' in Fig. 6) and associated dentition (referred to as m1–7 from mesial to distal; Figs 1, 2, 6), although the absolute tooth positions are unknown. Neither visible inspection nor CT data enabled us to determine whether interdental plates were present. The left maxilla is also partially medially exposed and preserves more of the posterior and dorsal parts, including the anteroventral border of the antorbital fenestra and fossa, and the base of the dorsal process (= ascending ramus, 'dp' in Fig. 6). Some of the maxillae are embedded in the matrix therefore we segmented the more complete left maxilla, but differentiation of the maxilla from other bones and matrix was difficult for the anterior edge, dorsal process and palatal contact because of poor density contrast in the CT scan slices. Neither maxilla is articulated with the surrounding bones, except for a laminar medial extension of the left maxilla that extends to inferred palatal remains ('?pal' in Fig. 6). The right maxilla appears to occlude with a portion of the right dentary (Fig. 1C, D).

In lateral view the anteroventral section of the left maxilla is missing, therefore the shape of the maxilla–premaxilla suture, whether a prenarial gap is present or absent, or whether the maxilla participates in the external naris, are not known. Furthermore, it is not clear whether the anterior proportion of the maxilla was anteriorly elongated like that of *Tawa hallae* (GR 241), *Daemonosaurus chauliodus* (CM 76821) and *Coelophysis bauri* (CM 31374) or anteriorly shorter like that of the herrerasaurids *Gnathovorax cabreirai* (CAPPA/UFSM 0009) and *Herrerasaurus ischigualastensis* (PVSJ 407). The broken edge of the maxilla along the dental margin exposes replacement teeth in the first three preserved alveoli (Figs 1, 6). More posteriorly, two consecutive alveoli host fully erupted teeth in preserved alveoli positions 4 and 5, and at least two more alveoli are present posterior to the erupted teeth. These empty alveoli are referred to as positions 6 and 7 (Fig. 6).

The maxilla bears a clear dorsal process, although some of it is obscured by the prefrontal in lateral view. The posterior edge of the base of the dorsal process forms the anteroventral portion of the antorbital fenestra and projects *c.* 60° posterodorsally relative to the main body of the maxilla. Although partially hidden, the dorsal process tapers, like that of dinosaurs such as *Herrerasaurus ischigualastensis* (PVSJ 407), *Tawa hallae* (GR 241) and *Coelophysis bauri* (CM 31374), but in contrast with the rectangular form in pseudosuchians such as *Postosuchus kirkpatricki* (TTU-P9000), *Dromicosuchus grallator* (NCSM 13733) and *Revueltosaurus callenderi* (PEFO 34274). A sliver of the anterior edge of the dorsal process of the maxilla of *Ptychotherates bucculentus* is preserved against the lateral edge of the preserved left nasal (Fig. 1), but we cannot be certain as to where along the rest of the process it is from, or how much bone lay between.

The posterolateral edge of the base of the dorsal process demarcates a well defined but small antorbital fossa ('afr' in Fig. 6), which is partially visible in lateral view, but also anteriorly invades the base of the process as a

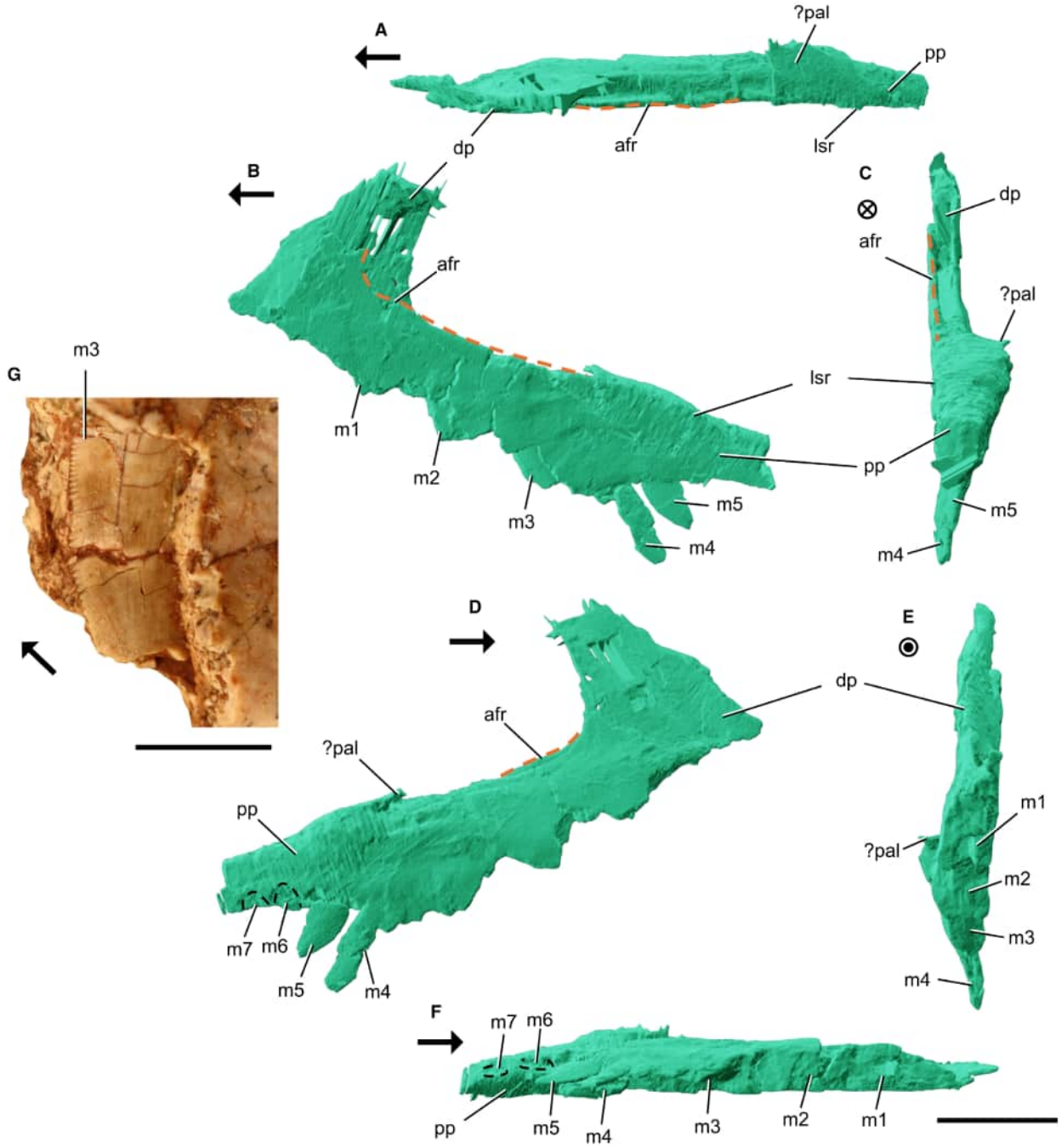

FIG. 6. The left maxilla of *Ptychotherates bucculentus* (CM 31368). A–F, digital reconstructions in: A, dorsal; B, lateral; C, posterior; D, medial; E, anterior; F, ventral view. G, a photograph of the third preserved erupted maxilla tooth in labial view. *Abbreviations*: afr, antorbital fossa rim; dp, dorsal process; lsr, lateral swelling ridge; m1–7, preserved maxillary tooth positions; pp, posterior process; ?pal, possible palatine. Arrows indicate anterior direction, crossed circle indicates posterior out of page and dotted circle indicates anterior out of page. Scale bars represent: 2 cm (A–F); 5 mm (G).

pocket. This antorbital fossa is similar to that of *Tawa hallae* (GR 241) and *Herrerasaurus ischigualastensis* (PVSJ 407) rather than the more laterally open fossa of neotheropods (e.g. *Zupaysaurus rougieri*, PULR-V 076; *Coelophysis bauri*, CM 31374) and early-diverging sauropodomorphs (e.g. *Eoraptor lunensis*, PVSJ 512; *Mbiresaurus raathi*, NHMZ 2222). We cannot resolve where the antorbital fossa terminates anteriorly, and it is difficult to distinguish replacement tooth alveoli from the antorbital fossa inside the dorsal process.

The antorbital fossa is laterally exposed at the base of the dorsal process, whereas the fossa is absent on nearly all of the lateral surface of the posterior process. The antorbital fossa is also restricted to the anterior portion of the maxilla in *Tawa hallae* (GR 241), *Daemonosaurus chauliodus* (CM 76821), and the herrerasaurids *Gnathovorax cabreirai* (CAPPA/UFSM 0009) and *Herrerasaurus ischigualastensis* (PVSJ 407). As a result of the lack of a laterally exposed antorbital fossa, there is no prominent ridge on the lateral surface of the maxilla as there is in silesaurids (*Silesaurus opolensis*, ZPAL Ab III/361, Dzik 2003), neotheropods (e.g. *Syntarsus katentakatae*, MNA V2623; *Coelophysis bauri*, CM 31374) and sauropodomorphs (e.g. *Eoraptor lunensis*, PVSJ 512; *Mbiresaurus raathi*, NHMZ 2222).

In lateral view, the angle between the ventral margin of the external antorbital fenestra (=dorsal margin of the posterior process) and the ventral margin of the posterior process is *c.* 35° to the horizontal, and this angle continues to the posterior termination of the element (Fig. 6). *Tawa hallae* (GR 241) and *Daemonosaurus chauliodus* (CM 76821) also have a similar tapering posterior process that tapers at a similar angle to the posterior termination of the maxilla. Herrerasaurids tend to have a similar angle anteriorly, such as *Herrerasaurus ischigualastensis* (PVSJ 407), *Gnathovorax cabreira* (CAPPA/UFSM 0009) and CAPPA/UFSM 11300 (Garcia *et al.* 2021), but the dorsal and ventral margins become parallel farther posteriorly in these taxa. In contrast, the dorsal and ventral margins of the posterior process are near-parallel in most other avemetatarsalians, such as lagerpetids (e.g. *Ixalerpeton polesinensis*, ULBRA-PVT059), silesaurids (e.g. *Asilisaurus kongwe*, NMT RB159), sauropodomorphs (e.g. *Eoraptor lunensis*, PVSJ 512) and neotheropods (e.g. *Coelophysis bauri*, CM 31374).

The posterior section of the posterior process of the left maxilla is triangular in coronal cross-section taken at the anteroposterior position of tooth m5. The dorsal surface swells slightly medially towards a planar, transversely oriented element that we interpret to be the palatine, although the exact form of this contact was difficult to interpret. The medial surface of the posterior portion of the right maxilla was not segmented because of poor contrast. Posteriorly, the dorsal edge of the maxilla has two major features. The more lateral surface forms a rounded ridge ('lsr' in Fig. 6), and the more medial bulbous part of the maxilla houses the more posterior alveoli. A few foramina are present on the lateral surface immediately dorsal to the ventral margin. The ventral edge of the posterior process of the maxilla is also slightly concave in lateral view, a shape seen also in *Herrerasaurus ischigualastensis* (PVSJ 407) and *Sanjuansaurus gordilloi* (PVSJ 605).

Nasal

Only the left nasal of *Ptychotherates bucculentus* is preserved (Figs 1, 7). The anterior portion with the perinarial processes is missing, but most of the medial and lateral edges are complete, except a few missing pieces on the thin edges, and the posterior process is largely intact where it would have met the other skull roof elements. The preserved position of the body of the nasal is angled *c.* 50° counterclockwise from the midline in dorsal view and shifted posteriorly over the frontals by at least 3 cm (Fig. 7A). The element was nearly completely reconstructed from CT data (Fig. 7), enabling three-dimensional reconstruction (Fig. 5). A mediolaterally oriented crack at the widest point of the preserved element resulted in an unnatural dorsal convexity in lateral view. There is also a slight ventral deflection ('vd' in Fig. 7) of *c.* 20° at the point across its length where the lateral portion starts to deepen dorsoventrally to form the posterodorsal border of the left naris. The underlying maxilla is cracked at the same point, therefore it is likely to be a taphonomic feature of bones being compressed against one another.

The nasal consists of a long, anteriorly tapering body that forms the dorsal region of the snout, and an anteriorly projecting process that expands ventrolaterally near its articulation with the maxilla and/or the premaxilla. The dorsal surface of the nasal is smooth with miniscule transversely oriented grooves on the dorsal surface, most conspicuously at the anterior end of the dorsolateral edge. The body of the nasal narrows transversely in the anterior direction. A rounded ridge ('lr' in Fig. 7) marks the dorsolateral edge of the nasal and, more anteriorly where the nasal expands ventrally, this ridge becomes more rounded. This lateral ridge is like that of *Tawa hallae* (GR 241) and some neotheropods such as *Coelophysis bauri* (Colbert 1989). The lateral ridge in *Ptychotherates bucculentus* and the aforementioned taxa contrasts with the more coronally rounder lateral margin in *Daemonosaurus chauliodus* (CM 76821) or herrerasaurids (e.g. *Herrerasaurus ischigualastensis*, PVSJ 407). Furthermore, the sharpness of the lateral ridge in *Ptychotherates bucculentus* is less pronounced than that of *Postosuchus kirkpatricki* (TTU-P9000) or *Batrachotomus kupferzellensis* (SMNS 52970). The ventral edge of the nasal articulated with the dorsal process of the maxilla, and a dorsal sliver of the maxilla is visible in dorsal view of the skull (Fig. 1A, B). A similar articulation surface between the nasal and maxilla is also present in *Tawa hallae* (GR 241) and *Herrerasaurus ischigualastensis* (PVSJ 407). The articulation surface between the nasal and maxilla in *Ptychotherates bucculentus* terminates at a large transverse crack (Fig. 7).

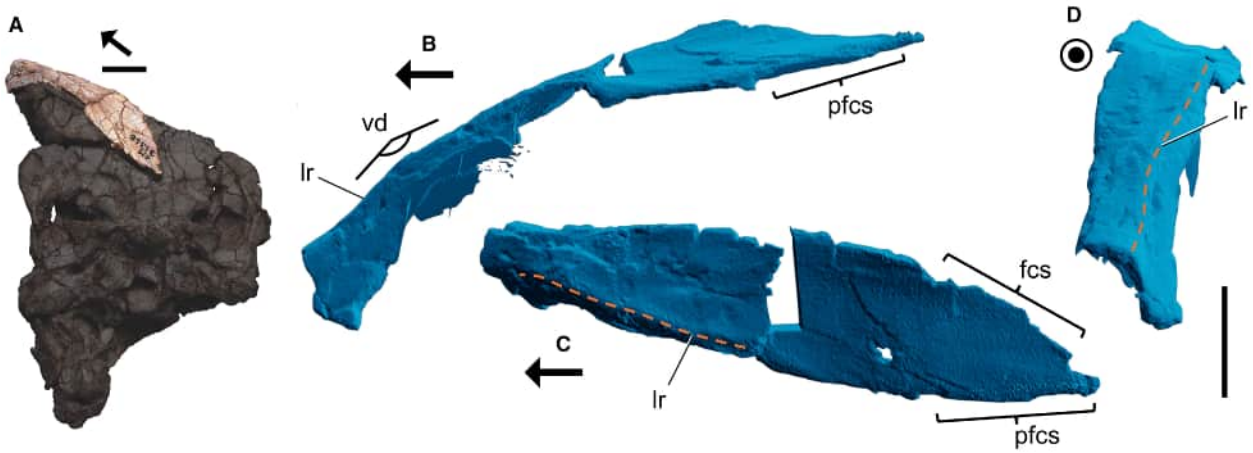

FIG. 7. The left nasal of *Ptychotherates bucculentus* (CM 31368). A, photograph of CM 31368 highlighting the left nasal in lateral view. B–D, digital reconstructions in: B, lateral; C, dorsal; D, anterior view. *Abbreviations*: fcs, frontal contact surface; lr, lateral ridge; pfcs, prefrontal contact surface; vd, ventral deflection. Arrow indicates anterior direction and dotted circle indicates anterior out of page. Scale bars represent 2 cm (A, B–D).

Anteriorly, the lateral portion of the nasal of *Ptychotherates bucculentus* is broken, hence its articulation with the premaxilla and how it formed the narial border are not clear. It is uncertain how far the nasal extended anteriorly, but what is preserved at the anteriormost end is *c.* 1.5 cm dorsoventrally tall. A slight lateral convexity begins to appear at the anterior end of the lateral surface, but it is not clear whether this is part of a narial fossa that extends from the external naris as in neotheropods (e.g. *Coelophysis bauri*, CM 31374). The midline suture is mostly intact and straight in dorsal view. The thickness of the midline articulation surface slightly deepens anteriorly.

Posteriorly, the nasal is largely intact but the thin nasal obscures details of the exact articulation surfaces with the prefrontal, lacrimal and frontal. The lateral ridge disappears at the presumed contact surface with the prefrontal ('pfcs' in Fig. 7), and the lateral ridge of the prefrontal is likely to be a continuation of the lateral ridge of the nasal through the lacrimal. The posterior end of the nasal tapers laterally, and we infer the medial edge of this region to be the frontal contact surface ('fcs' in Fig. 7). This indicates that the frontals had anterior processes that met on the midline to form a V-shaped projection. A similar configuration was inferred in *Herrerasaurus ischigualastensis* (Sereno & Novas 1994, fig. 1c) and in the neotheropod *Syntarsus kayentakatae* (MNA V2623) rather than the W-shaped suture in the tetanuran *Allosaurus fragilis* (Madsen 1976).

Prefrontal

Only the left prefrontal of *Ptychotherates bucculentus* (CM 31368) is preserved (Figs 1, 8). It is nearly complete, exposed everywhere but ventromedially, and was fully digitally reconstructed (Fig. 8). The preserved prefrontal of *Ptychotherates bucculentus* is disarticulated and angled anterolaterally like the nasal, but it is displaced posteriorly to a much lesser extent. As a result, it is preserved too far posterior relative to the frontal and too far anterior relative to the nasal.

The prefrontal is a distinct and prominent bone and is visible in lateral and dorsal views of the articulated skull (Fig. 5). These attributes are common for other Triassic saurischians such as *Herrerasaurus ischigualastensis* (PVSJ 407) and *Zupaysaurus rougieri* (PULR-V 076), but the prefrontal is repeatedly lost or obscured among more nested neotheropods, such as through fusion to the lacrimal as for *Velociraptor mongoliensis* (Smith-Paredes *et al.* 2018), or relative size reduction as for *Ceratosaurus nasicornis* (USNM 4735). The posteroventral edge of the prefrontal indicates that it formed part of the orbit.

Much like *Tawa hallae* (GR 241), the prefrontal of *Ptychotherates bucculentus* (CM 31368) is scalene triangular in dorsal view, with a long and straight medial edge and shorter posterolateral edge. The angle between the anterolateral and posterolateral edges in dorsal view is very close to the same angle in *Tawa hallae* (GR 241). In lateral view, the prefrontal of *Ptychotherates bucculentus* is almost T shaped, having a substantial anteroposteriorly oriented dorsal body and short ventral process ('vp' in Fig. 8) descending from the lateral edge. In lateral view the curvature of the posteroventral edge mirrors the anteroventral edge. This is in stark contrast to the preserved left prefrontal of *Saturnalia tupiniquim* (MCP-3845-PV) and articulated prefrontals of *Asilisaurus kongwe* (NMT RB15), which in lateral view resemble only the posterior half of the prefrontal of *Ptychotherates bucculentus* (CM

31368). The brittle anteroventral edge ('ae' in Fig. 8) is gently rounded with a concave edge in lateral view; this surface would have contacted the lacrimal as in other early dinosaurs. Although we cannot discern the contact relationships with the lacrimal, there is no notch on this edge of the prefrontal, therefore, no posterior process of the lacrimal invaded the prefrontal. A notch is also absent in *Tawa hallae* (GR 241) but not in *Herrerasaurus ischigualastensis* (PVSJ 407) or *Pampadromaeus barberenai* (ULBRA-PVT016).

The dorsal face of the prefrontal of *Ptychotherates bucculentus* is flat, similar to that of *Tawa hallae* (GR 241). The anteroventral and posteroventral edges of the prefrontal of *Ptychotherates bucculentus* meet at a ventral process that is triangular in lateral view. In lateral view this process projects orthogonally to the main body in the anteroposteriorly halfway point of the element, unlike the more anteriorly directed ventral process of the prefrontal of *Tawa hallae* (GR 241) or *Daemonosaurus chauliodus* (CM 76821). The ventral process is slightly anteriorly concave ('acv' in Fig. 8) in ventral view. The short ventral process has a rounded and acute tip, and we interpret this edge as complete or nearly complete. The ventral process is proportionally shorter than that of *Tawa hallae* (GR 241), for which it is longer than half the anteroposterior length of the entire prefrontal.

The posteroventral face of the prefrontal contributes to the anterodorsal edge of the orbit. We deduce from the relative size and morphology of the postorbital and frontal that the prefrontal forms the anterior third of the dorsal orbital boundary, more like most other early dinosaurs (e.g. *Tawa hallae*, GR 241; *Herrerasaurus ischigualastensis*, PVSJ 407) than in *Daemonosaurus chauliodus*, for which it forms half the dorsal orbit boundary (Nesbitt & Sues 2021). Along this edge of the element, only a laterally positioned ridge ('lpr' in Fig. 8) of a cross-sectional interior angle grading from 30° to 90° is exposed in CM 31368, but CT showed a more medially positioned ridge of a cross-sectional interior angle of *c.* 60°. This medial posteroventral edge is interpreted as the prefrontal expression of the crista cranii ('cc' in Fig. 8), thereby the space between the ridges contributes to the orbital fossa, although orientation of this medial ridge with the crista cranii preserved on the left frontal is difficult because the prefrontal–frontal articulation is not preserved.

Our digital reconstruction of the prefrontal also indicates a short process or ridge projecting off the centre of the ventral surface of the main dorsal body ('up,' Fig. 8), with an excavation bordering it posterolaterally that parallels the orbital fossa rim, but it is ambiguous whether this is a real anatomical feature with no known homologous structure in other closely related taxa, or a taphonomic artefact. The texture of the dorsal and lateral faces is smooth and lacks rugosity or grooves.

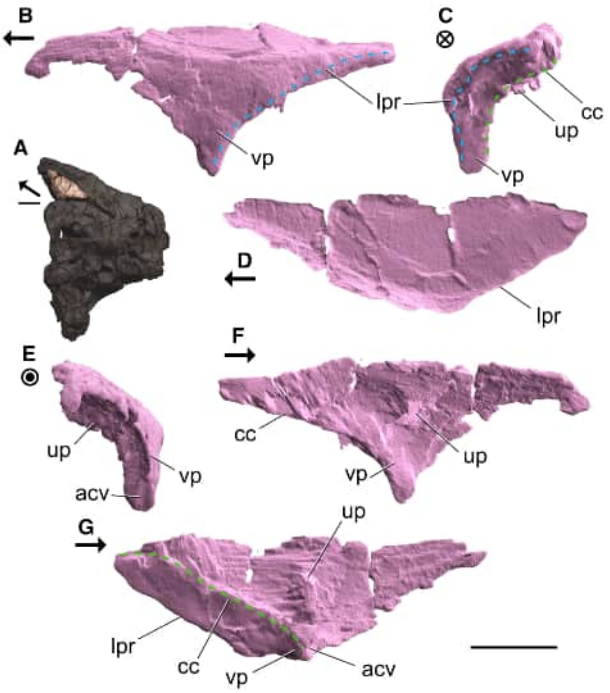

FIG. 8. The left prefrontal of *Ptychotherates bucculentus* (CM 31368). A, photograph of CM 31368 highlighting the left prefrontal in dorsal view. B–G, digital reconstructions in: B, lateral; C, posterior; D, dorsal; E, anterior; F, medial; G, ventral view. *Abbreviations*: acv, anterior concavity of the ventral process; cc, crista cranii; lpr, lateral posterior ridge; up, unidentified process; vp, ventral process. Arrows indicate anterior direction, crossed circle indicates posterior out of page, and dotted circle indicates anterior out of page. Scale bars represent 2 cm (A, B–G).

Frontal. Both frontals of *Ptychotherates bucculentus* are preserved but the anterior portion is missing in both elements, and parts of the bones are obscured by other elements (e.g. nasal) (Figs 1, 9, 10). We cannot reconstruct their total anteroposterior length because a fracture crosses the elements from the anterolateral end of the left frontal to the right frontal suture with the right postorbital. Each frontal is preserved in near articulation with the rest of the skull roof, particularly the postorbital posterolaterally and parietal posteriorly (Fig. 9). The suture at the midline is well defined, and a gap at the suture with the postorbital enables this contact to be fully described. The suture with the parietals is difficult to distinguish because of fractures in the area, although an estimate was made in the digital reconstruction (Fig. 9) based on a subtle crack in the CT data.

Dorsally, the frontal is flat across its preserved length, similar to that of *Tawa hallae* (GR 241), *Daemonosaurus chauliodus* (CM 76821), *Herrerasaurus ischigualastensis* (PVSJ 407) and *Coelophysis bauri* (CM 31374). The posterior portion bears a clear supratemporal fossa ('stfo' in Figs 9, 10) defined by a slight change in angle from the

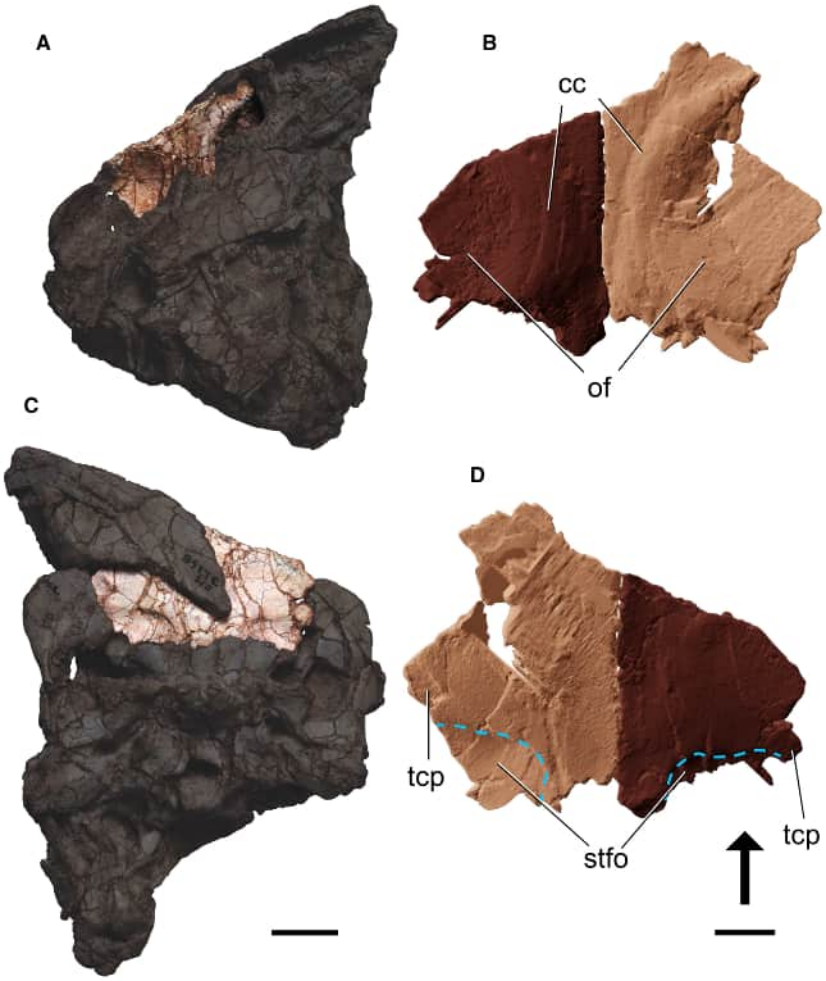

FIG. 9. The frontals of *Ptychotherates bucculentus* (CM 31369). A, C, photographs of CM 31368 with the frontals highlighted in: A, ventral; C, dorsal view. B, D, digital reconstructions of the frontals in: B, ventral; D, dorsal view. *Abbreviations*: cc, crista cranii; of, orbital fossa; stfo, supratemporal fossa; tcp, tab for contact with postorbital. Arrow indicates anterior. Scale bars represent: 2 cm (A, C); 1 cm (B, D).

dorsal surface, a character state found in all dinosaurs (Langer & Benton 2006). Posteriorly, the frontal meets the parietal in an interdigitating suture that is largely transversely oriented (Fig. 9).

The articulation between the frontal and postorbital is complex and distinct (Fig. 10). The posterolateral portion of the frontal meets the postorbital directly, so that the postfrontal is absent as in other dinosaurs (Langer & Benton 2006). At the anterior end of their contact, a lateral projection of bone of the frontal lies ventral to the postorbital, whereas a tab of bone of the frontal located immediately anterior to the supratemporal fossa lies over a depression on the dorsal surface of the postorbital ('tcp' in Fig. 9). Posteriorly, it appears that a flange of the postorbital lies on the dorsal surface of the frontal, but this is not as clear as the other parts of the articulation surface. A nearly exact configuration is present between the frontal and postorbital of *Tawa hallae* (GR 241). In *Herrerasaurus ischigualastensis* (PVSJ 407), the postorbital dorsally overlaps the frontal whereas in sauropodomorphs (*Mbiresaurus raathi*, NHMZ 2222, Griffin *et al.* 2022, fig. 2v) and neotheropods (e.g. *Coelophysis bauri*, CM 31374) an anterior projection of the postorbital fits into a distinct slot on the dorsal surface of the frontal.

Ventrally, the orbital fossa ('of' in Fig. 9) and crista cranii ('cc' in Fig. 9) of the left frontal are completely intact, showing that the cristae cranii of *Ptychotherates bucculentus* are low rounded ridges rather than a sharply defined ridge. This is unlike the sharp ridges on that of the early-diverging sauropodomorph *Saturnalia tupiniquim* (MCP 3845 PV) or the double ridge on the sauropodomorph *Panphagia protos* (PVSJ 874), but similar to *Tawa hallae* (GR 241), the dinosauriform *Asilisaurus kongwe* (NMT RB159) and the neotheropod '*Syntarsus*'

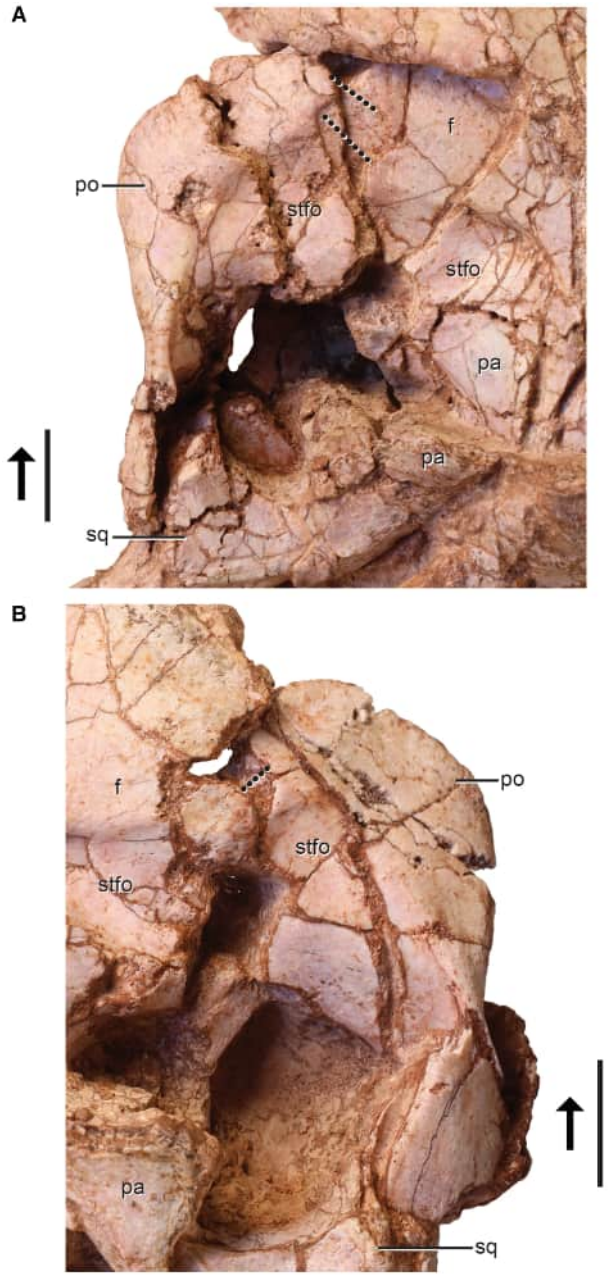

FIG. 10. The contact between the frontal and postorbital of *Ptychotherates bucculentus* (CM 31368) in dorsal view. A, the left postorbital is shifted anterolateral of its contact with the frontal as indicated by the articulation points connected by the dotted lines. B, the right postorbital is shifted anterolateral of its contact with the frontal as indicated by the articulation points connected by the dotted line. *Abbreviations*: f, frontal; pa, parietal; po, postorbital; sq, squamosal; stfo, supratemporal fossa. Arrow indicates anterior direction. Scale bars represent 1 cm.

rhodesiensis (NHMZ QG 193, Raath 1978). The posterior extent of the crista cranii appears to be at the suture with the parietals. The olfactory bulb fossae were broken away during preparation.

Parietal. Both parietals are present and remain in articulation with the surrounding bones, although their posterior extent is obscured by crushing and the dorsal overlap of the supraoccipital (Figs 1, 3, 10). The parietal of *Ptychotherates bucculentus* meets the frontal anteriorly at an interdigitating suture, the laterosphenoid at its anterolateral edge, and the anterior portion forms the posteromedial boundary of the supratemporal fossa. The supratemporal fossa continues from the frontal to the parietal, and the posterior extent of the fossa is not clear given that there is little demarcation of the fossa from the main body of the parietal. This is similar to *Tawa hallae* (GR 241), but unlike *Herrerasaurus ischigualastensis* (PVSJ 407), in which the fossa is separated by a distinct rim on the dorsolateral surface. It is clear that the dorsal exposure of the parietal of *Ptychotherates bucculentus* was nearly flat and that a sagittal crest was clearly absent.

The posterolateral process of the parietal was taphonomically slightly rotated anteriorly on its dorsal edge (Fig. 1), whereas this is typically a coronally oriented planar extension for other early-diverging dinosaurs (e.g. *Saturnalia tupiniquim*, MCP 3845 PV). The process extends laterally for about half the mediolateral length of the supratemporal fenestra. Dorsally, the posterolateral process terminates in a tab-like process (Figs 1, 10), and in posterior view a tapering ventrolateral process extends to contact the posteromedial edge of the squamosal. The dorsal tab-like process is also present in *Herrerasaurus ischigualastensis* (PVSJ 407). The ventral edge of the posterolateral process forms a large posttemporal opening with a long axis nearly as long as the width of the foramen magnum (Fig. 3).

Postorbital. Both postorbitals are nearly completely preserved and close to natural articulation with the other skull roof bones (Figs 1, 2, 10, 11). Between the left and right elements, we digitally reconstructed almost the entire element (as shown in red in Figs 5, 11). In lateral view, the postorbital of *Ptychotherates bucculentus* is tripartite with anterior, ventral and posterior processes. The postorbital has contacts with the frontal and laterosphenoid anteromedially, the squamosal posteromedially and the jugal ventrally. In lateral view, the postorbital forms the posterodorsal boundary of the orbit and anterodorsal boundary of the infratemporal fenestra. Dorsally, the postorbital comprises the anterolateral boundary of the supratemporal fenestra. The posteromedial region of the anterior process, about one-third of its area, is dorsally depressed, marking the supratemporal fossa (=frontoparietal fossa *sensu* Holliday *et al.* 2020; 'stfo' in Fig. 11).

The anterior process of the postorbital of *Ptychotherates bucculentus* has a broad, anteroposteriorly oriented contact with the frontal ('fcs' in Fig. 11). Anterior to the

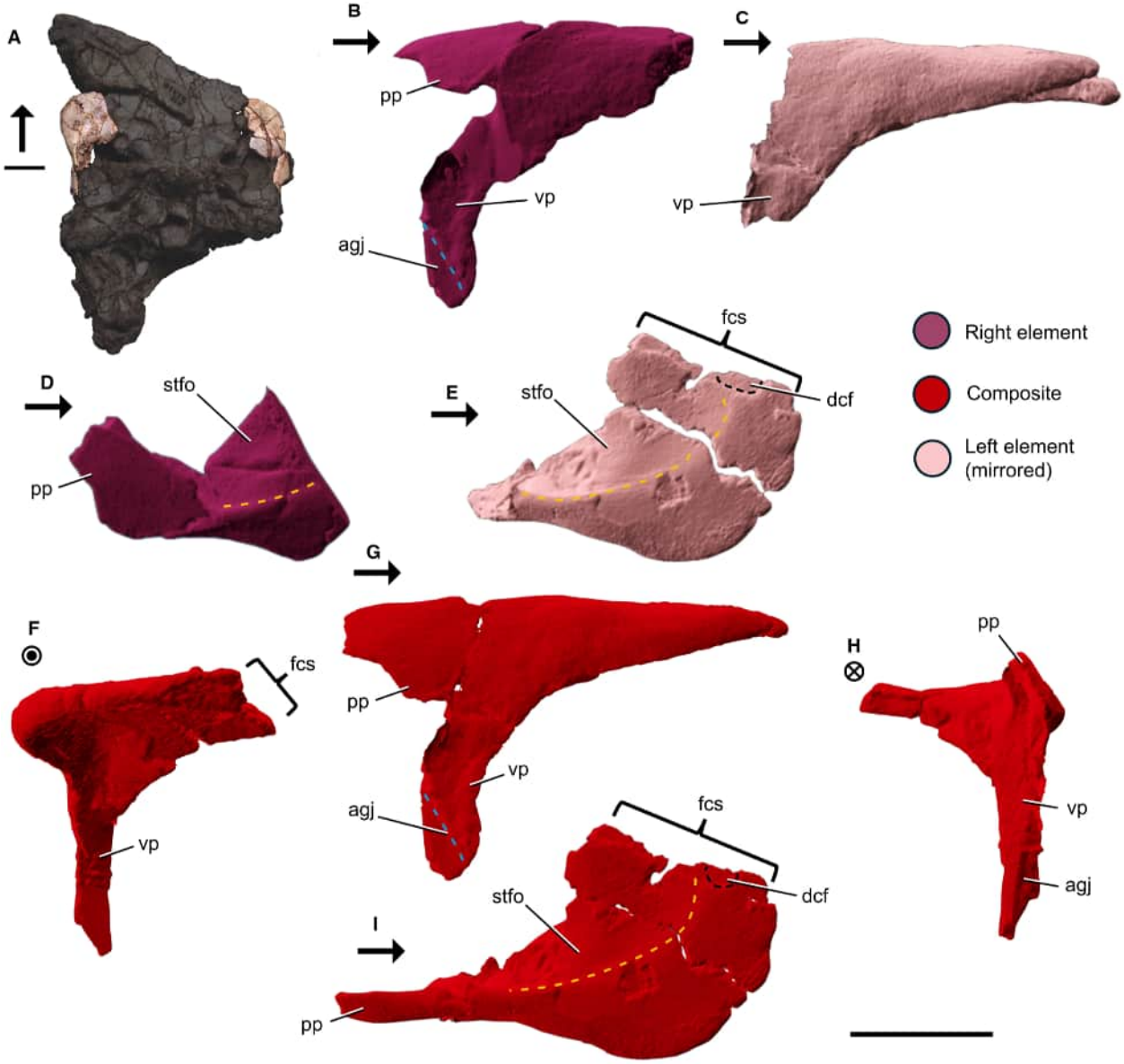

FIG. 11. The postorbitals of *Ptychotherates bucculentus* (CM 31368). A, photograph of CM 31368 highlighting the postorbitals in dorsal view. B, D, digital reconstructions in: B, lateral; D, dorsal view. C, E, mirrored digital reconstructions in: C, lateral; E, dorsal view. F–I, composite digital reconstructions of a hypothetical nearly complete right postorbital in: F, anterior; G, lateral; H, posterior; I, dorsal view. *Abbreviations*: agj, articulating groove for the jugal; dcf, depression for contact with the frontal; fcs, frontal contact surface; pp, posterior process; stfo, supratemporal fossa; vp, ventral process. Arrows indicate anterior direction, crossed circle indicates posterior out of page and dotted circle indicates anterior out of page. Scale bars represent 2 cm (A, B–I).

supratemporal fossa, the postorbital features a dorsal depression at its medial edge (Fig. 10, 'dcf' in Fig. 11) that appears anteroposteriorly aligned for contact with a similarly sized lateral tab of the frontal. No feature on either postorbital of *Ptychotherates bucculentus* suggests any substantial medial projections into the frontal (or anterior overlapping by the frontal), nor do the frontals show any receiving slots as present in sauropodomorphs (e.g. *Mbiresaurus raathi*, NHMZ 2222) and neotheropods (e.g. *Coelophysis bauri*, CM 31374). The anteroposterior orientation of the postorbital–frontal suture is similar to both *Herrerasaurus ischigualastensis* (Sereno & Novas 1994) and *Tawa hallae* (GR 241).

In dorsal view, the postorbital is hatchet shaped in that the posterior process is mediolaterally thin but the prominent anterior process is almost square and extends medially (Figs 10, 11). This hatchet shape, as well as the direction and form of the postorbital contact with the

frontal, are most similar to the postorbitals of *Tawa hallae* (GR 241) and *Daemonosaurus chauliodus* (CM 76821). By comparison, the anterior process of the postorbital for other Triassic dinosaurs is slender and tapering (e.g. *Coelophysis bauri*, CM 31374; *Zupaysaurus rougieri*, PULR-V 076; *Saturnalia tupiniquim*, MCP-3845-PV).

The anterolateral portion of the postorbital of *Ptychotherates bucculentus* (CM 31368) overhangs the dorsal portion of the orbit, similar to that of *Tawa hallae* (GR 241) and *Daemonosaurus chauliodus* (CM 76821) (Figs 1, 5). Other early-diverging dinosaurs have an anterolaterally projecting flange that protrudes into the orbits in lateral view (e.g. *Herrerasaurus ischigualastensis*, PVSJ 407; *Eoraptor lunensis*, PVSJ 512; *Pampadromaeus barberenai*, ULBRA-PVT016), but these features occur between the anterior and ventral processes, rather than being entirely a feature of the anterior process, hence they do not appear to be the same feature as that of *Ptychotherates bucculentus* (CM 31368), *Tawa hallae* (GR 241) and *Daemonosaurus chauliodus* (CM 76821).

The rim surrounding the supratemporal fossa continues posteriorly into the dorsal edge of the posterior part of the postorbital, as the element narrows mediolaterally and deepens dorsoventrally between the anterior and posterior regions. The posterior process ('pp' in Fig. 11) fits into a congruent depression on the dorsolateral surface of the anterior process of the squamosal (Fig. 5, also see description of the squamosal). In dorsal view, the squamosal precludes the posterior process of the postorbital from participation in the supratemporal fenestra. The postorbital may also have had a close or point contact with the parietal anterior to the supratemporal fenestra, as in *Herrerasaurus ischigualastensis* (PVSJ 407), but this region is slightly damaged (Figs 1, 3).

The ventral process of the postorbital is more complete on the right side, and its posteroventral border has a groove that possibly formed a tongue-in-groove contact with the dorsal process of the jugal ('agj' in Fig. 11). The jugal–postorbital junction of *Tawa hallae* (GR 241) is similar, but whereas the small ridge bounding this depression anteriorly is rounded in *Ptychotherates bucculentus* (CM 31368), it is sharper and more pronounced in *Tawa hallae* (GR 241).

Squamosal. The triaxial squamosal is well preserved on both sides, except the end of the ventral process, which is fractured and mostly missing (Figs 1, 3, 12, 13). A fragment of the ventral process of the left squamosal is preserved disarticulated and projecting through a fractured region of the left jugal (Fig. 2). Both squamosals are in articulation with the postorbital anterolaterally, the quadrate posteroventrally, the parietal posteromedially and the otoccipital of the braincase posteriorly. The parietal is in contact, but the articulating regions of both parietals are

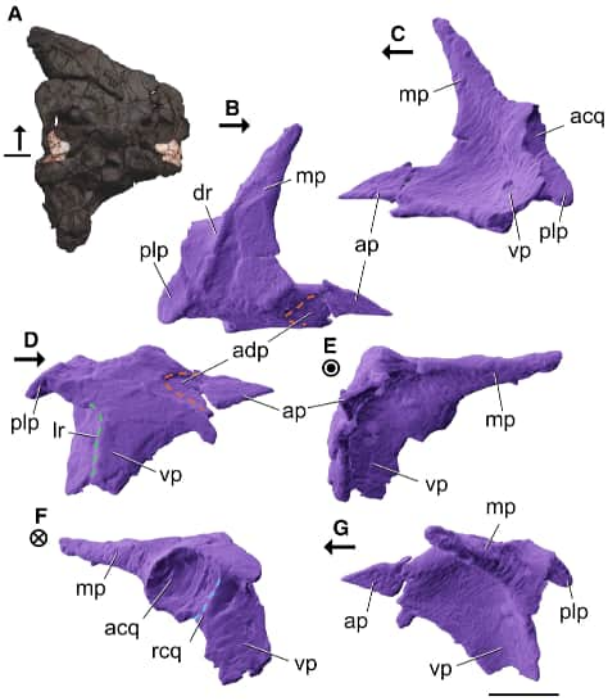

FIG. 12. The squamosals of *Ptychotherates bucculentus* (CM 31368). A, photograph of CM 31368 highlighting the squamosals in dorsal view. B–G, digital reconstructions of the right squamosal in: B, dorsal; C, ventral; D, lateral; E, anterior; F, posterior; G, medial view. *Abbreviations*: ap, anterior process; acq, articular cotylus for the quadrate; adp, articular depression for the postorbital; dr, dorsal ridge; lr, lateral ridge; mp, medial process; plp, posterolateral process; vp, ventral process. Arrows indicate anterior direction, crossed circle indicates posterior out of page and dotted circle indicates anterior out of page. Scale bars represent: 2 cm (A); 1 cm (B–G).

disarticulated from the main parietal body contacting the frontal. The squamosal articulation with the quadratojugal ventrally cannot be assessed because of breakage in both elements.

The blade-like anterior process ('ap' in Fig. 12) tapers anteriorly and is exceptionally thin in dorsomedial view, owing to a lenticular lateral depression ('adp' in Fig. 12) that receives the posterior process of the postorbital (Figs 1, 5, 13). A similar lateral overlap of the squamosal by the postorbital is present in *Herrerasaurus ischigualastensis* (PVSJ 407) and *Tawa hallae* (GR 241, GR 1088), whereas in sauropodomorphs (e.g. *Saturnalia tupiniquim*, MCP-3845-PV; *Plateosaurus trossingensis*, MSF 16.1) and neotheropods ('*Syntarsus*' *rhodesiensis*, NHMZ QG 193, NHMZ QG 194; *Allosaurus fragilis*, Madsen 1976) a tongue-in-groove condition with a dorsoventrally narrower process is present.

In dorsal view, the anteromedial edge of the squamosal of *Ptychotherates bucculentus* forms the lateral border of

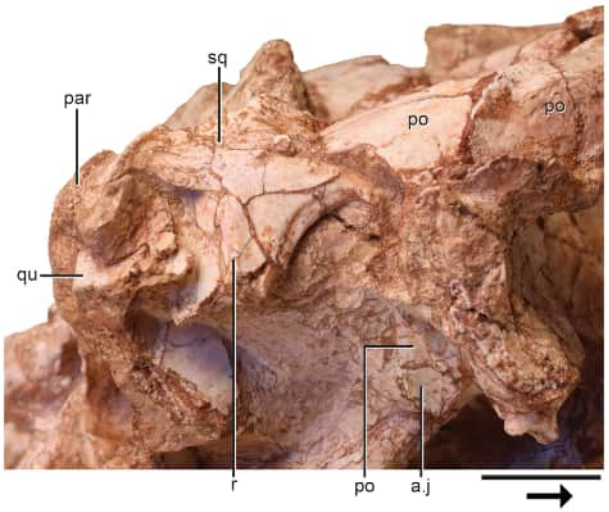

FIG. 13. Close-up view of the right squamosal and surrounding bones of *Ptychotherates bucculentus* (CM 31368) in left lateral view. *Abbreviations*: a., articulates with; j, jugal; par, paroccipital process of the otoccipital; po, postorbital; qu, quadrate; r, ridge; sq, squamosal. Arrow indicates anterior direction relative to squamosal. Scale bar represents 1 cm.

the supratemporal fenestra whereas the tapering medial process ('mp' in Fig. 12) contributes to the posterior border of the supratemporal fenestra. Unlike *Tawa hallae* (GR 241), the medial process of the squamosal of *Ptychotherates bucculentus* curves slightly anteriorly. The posterior edge of the medial process transitions laterally into a distinct dorsal ridge ('dr' in Fig. 12) that marks the posterior edge of the supratemporal fossa. This defined ridge curves anterolaterally where it nearly contacts the postorbital. *Tawa hallae* (GR 241) has a similar ridge that is situated farther posteriorly on the squamosal. In the supratemporal fossa, the surface of the squamosal is slightly concave. By contrast, the squamosal of *Herrerasaurus ischigualastensis* (PVSJ 407) lacks any supratemporal fossa.

The posterolateral process ('plp' in Fig. 12) of the squamosal of *Ptychotherates bucculentus* is complete on both sides. The process contacts the paroccipital process of the braincase, which extends slightly laterally beyond the squamosal as in some other early dinosaurs, such as *Herrerasaurus ischigualastensis* (PVSJ 407). The posterolateral process extends laterally in *Ptychotherates bucculentus* as in *Tawa hallae* (GR 241), which contrasts with the posteriorly oriented prong of *Saturnalia tupiniquim* (MCP-3845-PV).

The articular cotylus with the quadrate head ('acq' in Fig. 12) is anteromedially concave. Like *Tawa hallae* (GR 241), a rim forms the posterior edge of the posterolateral process and transitions ventrally into the posterior edge of the ventral process. Subtle lateral emargination of the cotylus by a dorsoventrally oriented rim ('rcq' in Fig. 12) resembles *Tawa hallae* (GR 241), and ventral to that is the posterolateral surface of the ventral process. The orientation of the cotylus of the squamosal indicates that the dorsal portion of the quadrate was fully visible in lateral view (Figs 5, 13), like that of other dinosaurs (Langer & Benton 2006).

In lateral view, the ventral process is divided by a dorsoventrally oriented ridge ('lr' in Fig. 12) that divides the surface into a posterolateral surface and a lateral surface. The squamosal of *Herrerasaurus ischigualastensis* (PVSJ 407) possesses the same ridge on the lateral surface of the ventral process, and this ridge divides an anterolateral surface from a posterolateral depression, an autapomorphy of the taxon as stated by Sereno & Novas (1994). As a result, both *Herrerasaurus ischigualastensis* and *Ptychotherates bucculentus* have wide ventral processes. The posterolateral surface of *Ptychotherates bucculentus* is more posteriorly directed than the more laterally positioned feature in *Herrerasaurus ischigualastensis*. Neotheropods (e.g. *Coelophysis bauri*, CM 31374; '*Syntarsus*' *rhodesiensis*, Raath 1978, fig. 4m based on NHMZ QG 193 and QG 194) and the ornithischian *Heterodontosaurus tucki* (SAM-PK-K337, SAM-PK-K1332) have a distinct lateral ridge continuous with the lateral edge of the postorbital; this ridge is absent in *Tawa hallae* (GR 241) and *Ptychotherates bucculentus* (CM 31368). The anterior edge of the ventral process also has a slight embayment that follows the edge ventrally (Fig. 12).

The angle between the ventral and anterior processes of the squamosal in lateral view in *Ptychotherates bucculentus* is slightly obtuse, more similar to *Tawa hallae* (GR 241) and '*Syntarsus*' *rhodesiensis* (Raath 1978, fig. 4m, based on NHMZ QG 193 and NHMZ QG 194) than to the acute angle of *Saturnalia tupiniquim* (MCP-3845-PV). Anteromedial and ventral views of the reconstructed squamosal show a concavity for the infratemporal opening, similar to *Tawa hallae* (GR 241) and *Saturnalia tupiniquim* (MCP-3845-PV).

Jugal. The large and mediolaterally thin left jugal of *Ptychotherates bucculentus* (CM 31368) is mostly preserved (Figs 2, 5, 14). The tip of the dorsal (=postorbital) process ('dp' in Fig. 14), the ventral boundary of the orbit, and anterior process that contacted the lacrimal and maxilla are incomplete. Our digital reconstruction of the element showed that the externally visible anterior extent of the element is also the extent of preservation, abutting unnaturally against the lateral surface of the maxilla and obscuring the jugal–maxilla contact. Reconstruction using CT data also clarified the configuration of its posterior articulation with the quadratojugal (Fig. 5). The posterior edge of the ventral process of the postorbital (Figs 11, 13) implies a long and slanted joint between it and the jugal

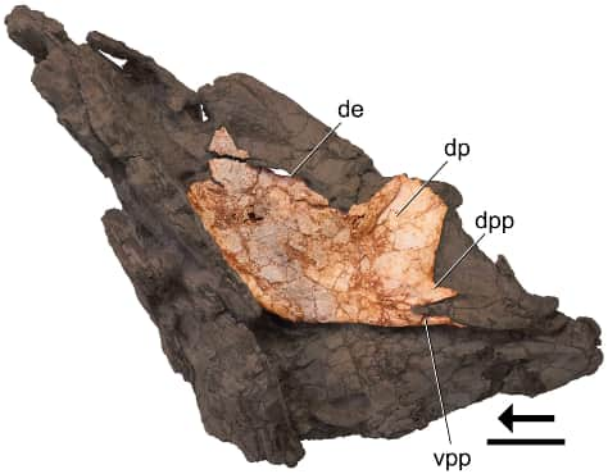

FIG. 14. Photograph of CM 31368 highlighting the left jugal of *Ptychotherates bucculentus* in lateral view. *Abbreviations*: de, dorsal embayment; dp, dorsal process; dpp, dorsal posterior process; vpp, ventral posterior process. Arrow indicates anterior direction. Scale bar represents 2 cm.

when viewed laterally, consistent with other dinosaurs (e.g. *Eoraptor lunensis*, PVSJ 512; *Heterodontosaurus tucki*, SAM-PK-K1332), although the corresponding dorsal tip of the dorsal process of the jugal is broken.

The depth of the jugal ventral to the orbit is proportionally greater than that in any known Triassic ornithodiran (Table 1). The anterodorsal edge of the jugal, which would have formed the ventral edge of the orbit, is broken by crushing of other skull elements; nevertheless, enough of a finished dorsal margin is preserved to ascertain that the height of the jugal ventral to the base of the orbit was at least 29 mm. This jugal depth is at least three times the dorsoventral height of the posterior process of the jugal (measured at the anteriormost part of the posterior process or the base of the process), greater than half the dorsoventral height of the quadrate shaft, and close to the length of the ventral process of the postorbital (measured from the ventral tip to the dorsal top of the element in lateral view) (Table 1). *Tawa hallae* (GR 241) also has a relatively tall jugal, which is more than one-third the dorsoventral height of the orbit; this dorsal expansion of the jugal body is a synapomorphy of *Tawa hallae* and *Ptychotherates bucculentus*, but the depth of the jugal of *Ptychotherates bucculentus* still exceeds that of the proportions of *Tawa hallae* (Table 1). In all of these respects, the jugal of *Ptychotherates bucculentus* contrasts with the relatively slender jugals of neotheropods (e.g. *Coelophysis bauri*, CM 31374; *Zupaysaurus rougieri*, PULR-V 076) and sauropodomorphs (*Pampadromaeus barberenai*, ULBRA-PVT016) (Table 1). Relative to the height of the orbit, the jugal of the herrerasaurids (e.g. *Herrerasaurus ischigualastensis*, PVSJ 407) and *Daemonosaurus chauliodus* (CM 76821) is deeper than that of neotheropods and sauropodomorphs, but not nearly as deep as that of *Ptychotherates bucculentus* (Table 1).

The posterior process of the jugal of *Ptychotherates bucculentus* is deeply bifurcated into dorsal ('dpp' in Fig. 14) and ventral projections ('vpp' in Fig. 14) at its articulation with the quadratojugal (Figs 2, 5, 14). The slot between the prongs is V shaped in lateral view, and it receives the anterior process of the quadratojugal, a character state found in dinosaurs (Langer & Benton 2006). In lateral view the articulation surface with the quadratojugal extends anteriorly past the posterior edge of the dorsal process of the jugal, a character state seen broadly among saurischians such as *Tawa hallae* (GR 241) and *Daemonosaurus chauliodus* (CM 76821), as well as most neotheropods (e.g. *Coelophysis bauri*, CM 31374; *Zupaysaurus rougieri*, PULR-V 076). Notably, the V-shaped slot in the jugal of the sauropodomorph *Pampadromaeus barberenai* (ULBRA-PVT-016) reaches as far as the dorsal ramus of the jugal, possibly hinting at a wider distribution of the character state among early-diverging saurischians. In *Ptychotherates bucculentus* the dorsal edge of the posterior process of the jugal forms the anteroventral border of the infratemporal fenestra.

The jugal of *Ptychotherates bucculentus* lacks any ridges or ornamentation on its lateral surface. This is in contrast to taxa with an anteroposteriorly oriented ridge on the lateral surface such as herrerasaurids (e.g. *Gnathovorax cabreirai*, CAPPA/UFSM 0009), *Daemonosaurus chauliodus* (CM 76821), sauropodomorphs (e.g. *Eoraptor lunensis*, PVSJ 512) or neotheropods (e.g. *Coelophysis bauri*, CM 31374). The ventral edge of the jugal of *Ptychotherates bucculentus* is subtly convex in lateral view. The ventral edge posterior to its articulation with the maxilla is straighter in *Herrerasaurus ischigualastensis* (PVSJ 407) and *Daemonosaurus chauliodus* (CM 76821), but the ventral bowing of the jugal of *Ptychotherates bucculentus* (CM 31368) is nearly identical to that of *Tawa hallae* (GR 241). Anteriorly, this edge continues to curve dorsally and contacts with the posterodorsal edge of the maxilla.

The anterior process of the jugal expands dorsally; this dorsal expansion is also present in *Tawa hallae* (GR 241), *Herrerasaurus ischigualastensis* (PVSJ 407), *Gnathovorax cabreirai* (Pacheco *et al.* 2019) and the large neotheropod *Dilophosaurus wetherilli* (Marsh & Rowe 2020), whereas the anterior process narrows in *Daemonosaurus chauliodus* (CM 76821), the sauropodomorphs *Eoraptor lunensis* (PVSJ 512) and *Plateosaurus* (AMNH FARB 6810), and smaller neotheropods (e.g. *Coelophysis bauri*, CM 31374). A slight embayment ('de' in Fig. 14) on the lateral surface at the dorsal margin may mark its articulation with the lacrimal, but most of this area is broken (Figs 2, 14). The anterior process appears flat with no indication that the

element participated in the antorbital fossa, as in *Herrerasaurus ischigualastensis* (PVSJ 407), and due to the ambiguity of the jugal–lacrimal contact, it is not clear whether the jugal of *Ptychotherates bucculentus* participated in the antorbital fenestra like that of *Daemonosaurus chauliodus* (CM 76821). In ventral view the preserved jugal is sigmoidal, being medially concave at the quadratojugal juncture and ventral to the dorsal process, and medially convex anteriorly to that. This shape echoes the dorsal profile of the surangular, although both elements may have been taphonomically deformed together.

Quadratojugal. The quadratojugal of *Ptychotherates bucculentus* (CM 31368) is partially preserved on the left side and absent from the right (Figs 1–3, 5). The left element is in near articulation with the quadrate and forms the posteroventral corner and the ventral half of the posterior border of the infratemporal fenestra. The main body of the quadratojugal preserves anterior and dorsal processes, the latter missing the lateral and medial edges due to bone loss during preparation. In lateral view, the anterior process fits between a bifurcated posterior process of the jugal, as in other saurischian dinosaurs (Langer & Benton 2006). The anterior process of the quadratojugal extends anterior of the infratemporal fenestra as in *Tawa hallae* (GR 241), *Daemonosaurus chauliodus* (CM 76821) and neotheropods (e.g. *Coelophysis bauri*, CM 31374; *Zupaysaurus rougieri*, PULR-V 076; *Dilophosaurus wetherilli*, UCMP 37302), whereas the homologous process extends only about half the anteroposterior length of the jugal–quadratojugal bar in the herrerasaurids *Herrerasaurus ischigualastensis* (PVSJ 407) and *Gnathovorax cabreirai* (CAPPA/UFSM 0009), as well as in the early-diverging sauropodomorph *Eoraptor lunensis* (PVSJ 512).

The dorsal process seems to preserve the original height of the element, which currently terminates under the right paroccipital process of the braincase (Figs 1, 3). The dorsal process meets the anterior process at a 60–70° angle (to horizontal) so that the dorsal process is slanted anterodorsally. The main surface of the dorsal process is oriented posteriorly and is wide like that of *Tawa hallae* (GR 241). The posterior portion of the quadratojugal has a small posteriorly directed process with a blunt end that extends to the posteroventral end of the quadrate (Figs 2, 5).

Quadrate. The left quadrate is nearly complete and in articulation with the squamosal and otoccipital at its dorsal margin and with the articular, prearticular and surangular ventrally (Figs 1, 3, 5, 15, 16). Of the right quadrate, only the dorsal part is preserved in articulation with the squamosal (Fig. 13), whereas other parts of the pterygoid process are potentially also preserved but disarticulated. The left quadrate is exposed in posterior view

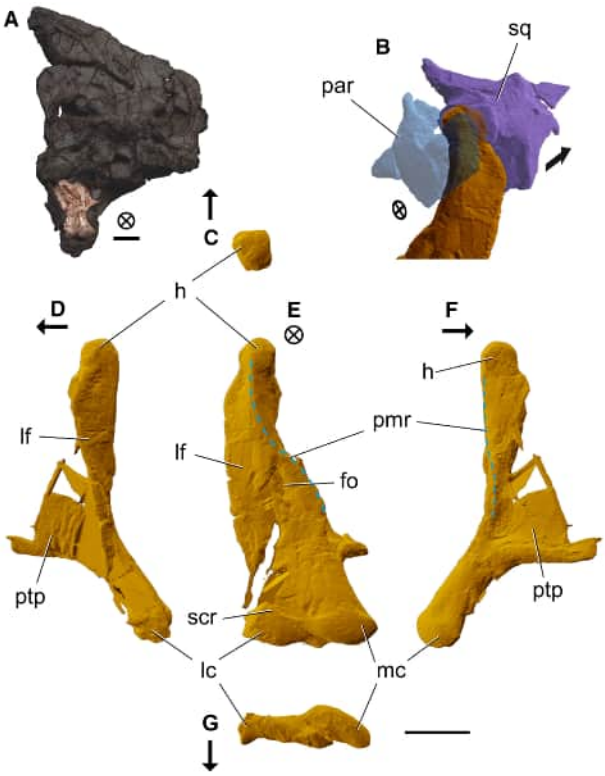

FIG. 15. The left quadrate of *Ptychotherates bucculentus* in various views. A, photograph of CM 31368 highlighting the left quadrate in posterior view. B, digital reconstruction of the quadrate head articulation between the paroccipital process and squamosal in oblique dorso-posterolateral view. C–G, digital reconstructions in: C, dorsal (isolated head); D, lateral; E, posterior; F, medial; G, ventral (isolated articular condyles) view. *Abbreviations*: fo, fossa; h, head; lc, lateral condyle; lf, lateral flange; mc, medial condyle; par, paroccipital process of the otoccipital; pmr, posteromedial ridge; ptp, pterygoid process; scr, supra-condylar ridge; sq, squamosal. Arrows indicate anterior direction and crossed circle indicates posterior out of page. Scale bars represent: 2 cm (A); 1 cm (B–G).

except for its head ('h' in Fig. 15), which was reconstructed from CT data. Although still largely articulated, the entire left quadrate rotated *c.* 60° from its natural position, such that it is seen in 'posterior' view when the majority of the skull roof is in 'dorsal' view (Figs 1, 16). The element may also be plastically deformed, but we cannot know how much therefore this was not altered in the reconstruction.

The dorsal head of the quadrate is rounded on its dorsal surface and is more circular in dorsal outline than that of the oval shape in *Tawa hallae* (GR 241). The main body is formed predominantly by a dorsoventrally oriented strip of bone and the base of an anteromedially projecting pterygoid process. The dorsal half of the main body appears laterally arched in posterior view, more so

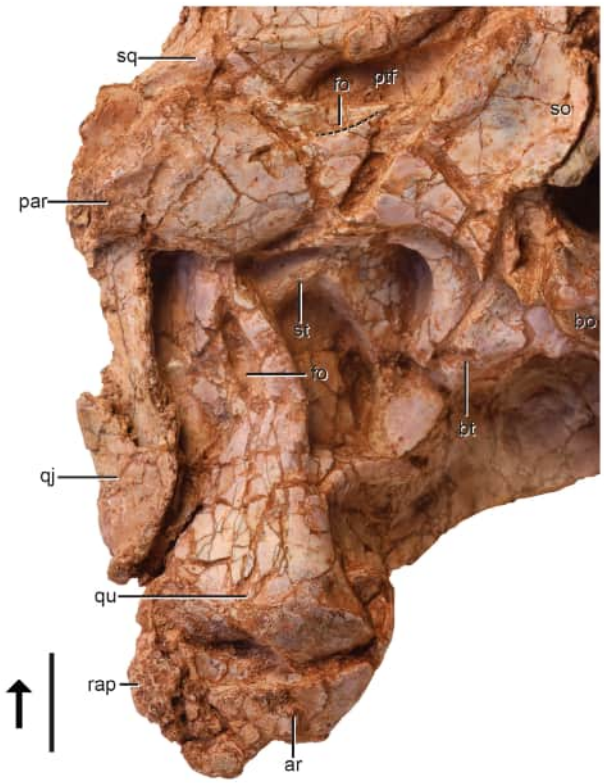

FIG. 16. The posterior surface of the left quadrate and surrounding bones of *Ptychotherates bucculentus* (CM 31368) in posterior view. *Abbreviations*: ar, articular; bo, basioccipital; bt, basituber; fo, fossa; pa, parietal; par, paroccipital process of the otoccipital; ptf, posttemporal fenestra; qj, quadratojugal; qu, quadrate; rap, retroarticular process; so, supraoccipital; sq, squamosal; st, stapes. Arrow indicates anterior direction relative to braincase. Scale bar represents 1 cm.

than in *Tawa hallae* (GR 241) or *Herrerasaurus ischigualastensis* (PVSJ 407), but this may be due to the aforementioned deformation of the element. The quadrate possesses a thin lateral flange ('lf' in Fig. 15) that tapers and twists anteriorly towards the head, and appears to continue ventrally to the ventral articular condyles. That region was not successfully reconstructed from the CT data, and it is obscured by the quadratojugal as preserved. The ventral centimetre-long segment of the main body is inclined 30° from the rest of the main body, and broadens mediolaterally into a medial condyle ('mc' in Fig. 15) and lateral condyle ('lc' in Fig. 15) to form the jaw joint with the articular. A posterolateral–anteromedially oriented groove lies between them on the ventral surface, and the medial condyle appears slightly larger and extends slightly more ventral than the lateral condyle. Similarly to *Tawa hallae* (GR 241), the lateral condyle appears to be anteriorly concave in ventral view, unlike the almost convex medial condyle. A subtle supracondylar ridge ('scr' in Fig. 15) outlines the two dorsally in posterior view.

In medial view, the medial edge of the medial condyle is continuous dorsally with a posteromedial ridge ('pmr' in Fig. 15) and the ventromedial edge of the pterygoid process ('ptp' in Fig. 15). The posteromedial ridge twists posterodorsally, appearing sigmoidal in posterior view (Fig. 15), and forms a dorsoventral crest on the posterior side of the quadrate head. At about the dorsoventral midheight of the main body, a dorsoventrally long depression is present ('fo' in Figs 15, 16) on the posterior surface. It appears that this does not pierce the bone, but is instead a deep depression. The quadrate of *Tawa hallae* (GR 241) also has the same depression in the same spot, a character state that appears unique to these two taxa given that it is absent in other closely related taxa (e.g. *Herrerasaurus ischigualastensis*, PVSJ 407; Appendix S1). It is not clear whether *Ptychotherates bucculentus* possesses a foramen on its lateral border with the quadratojugal, like that of *Herrerasaurus ischigualastensis* (Sereno & Novas 1994).

Pterygoid. A partial pterygoid is present but mostly obscured by other elements (Figs 1, 2). The ventral surface is exposed in external view with a partial lateral process and the region immediately ventral to the articulation with the pterygoid process of the braincase. The ventral surface of this region is concave with an extension dorsally where the pterygoid is constricted. A ridge defines the posterior edge of the lateral process. Unlike *Eoraptor lunensis* (PVSJ 512), no teeth are present on the ventral surface of the pterygoid.

Braincase. The braincase of *Ptychotherates bucculentus* is largely intact and exposed in posterior view and partially in ventral view (Figs 1, 3, 16). In posterior view, the braincase remains nearly symmetrical across the midline with a slight plastic shear such that the right portion is stretched dorsally relative to the left, but compression on an anteroventral–posterodorsal axis has rendered the posterior face of the braincase at a much closer orientation to that of the skull roof. The braincase is further distorted by compression of the supraoccipital into the brain cavity and the flattening of the paroccipital process, so that they are directed only laterally and not posterolaterally, like those of other dinosaurs with less compressed skulls (e.g. *Gnathovorax cabreirai*, CAPPA/UFSM 0009; '*Syntarsus*' *kayentakatae*, MNA V2623).

The basioccipital is largely intact (Figs 1, 3). The occipital condyle extends posterior of the rest of the braincase and has a well-defined rim on the ventral surface. In posterior view, the occipital condyle is bean shaped, and the suture with the exoccipital portion of the occipital condyle cannot be recognized, but only as a slight change in angle. The well-sutured exoccipital components of the

otoccipitals (=co-ossified opisthotic and exoccipital) are only slightly separated at the midline like that of *Gnathovorax cabreirai* (CAPPA/UFSM 0009), but in contrast to those of *Tawa hallae* (GR 241), *Daemonosaurus chauliodus* (CM 76821), and nearly all dinosaurs (Langer & Benton 2006) with widely separated exoccipitals. The obliteration of the exoccipital–basioccipital suture may be related to an older ontogenetic status in *Ptychotherates bucculentus*, but this one co-ossification feature is not reliable for ontogenetic status in reptiles (Griffin *et al.* 2021). Ventrally, the basioccipital is divided at the midline by a small cleft between symmetrical rounded projections (Fig. 3). This cleft is much shallower in *Ptychotherates bucculentus* compared with that of *Gnathovorax cabreirai* (CAPPA/UFSM 0009) and *Tawa hallae* (GR 241). A shallow depression is present ventrolateral of the occipital condyle, but it is far less defined than the rimmed depression of *Gnathovorax cabreirai* (CAPPA/UFSM 0009). The basitubera are only subtly represented by low knobs in *Ptychotherates bucculentus*. No suture is visible between the basioccipital and the parabasisphenoid on the ventral surface.

Both otoccipitals are nearly completely preserved, except the lateral end of the right paroccipital process. Both are exposed posteriorly, although structures anterior to the ventral process (=crista interfenestralis) are hidden from view and unable to be digitally reconstructed with confidence. The otoccipitals are in articulation with the squamosal anterolaterally, the basioccipital medially and ventrally, and the supraoccipital medially. They form the ventral border of the large posttemporal fenestrae (Figs 1, 3, 16) and the lateral walls of the foramen magnum. Like many bones in the specimen, the otoccipitals are riddled with cracks that hide sutures. Therefore, the otoccipital–supraoccipital suture, the otoccipital–basioccipital suture and otoccipital–parabasisphenoid suture cannot be seen.

Two exits of cranial nerve XII pass through the exoccipital component of the otoccipital and these are visible only in the brain cavity. The more posterior exit for this cranial nerve has a larger diameter than the more anterior one. Lateral to the otoccipital–occipital condyle contact, deep pockets represent the lateral component of the metotic foramen, although no other details can be seen. The posterior wall of the metotic foramen is a large ventral process of the otoccipital (Fig. 16) that extends ventral of the occipital condyle and attaches to the lateral side of the basioccipital. This laterally extensive ventral process hides the fenestra ovalis in posterior view, as in *Gnathovorax cabreirai* (CAPPA/UFSM 0009), *Tawa hallae* (GR 241), *Daemonosaurus chauliodus* (CM 76821) and the sauropodomorphs *Buriolestes schultzi* (CAPPA/UFSM 0035) and *Saturnalia tupiniquim* (MCP-3845-PV).

The paroccipital process expands dorsally and ventrally lateral of the midline to become paddle shaped in posterior view, similar to other early-diverging saurischians (e.g. *Gnathovorax cabreirai*, CAPPA/UFSM 0009). The paroccipital process is broadest immediately posterior to the head of the quadrate and narrows ventrolaterally to a rounded point at its lateral extent. The paroccipital process is mediolaterally 42 mm long from the foramen magnum to its lateral end, and 12 mm tall at its dorsoventrally deepest point immediately posterior to the quadrate head, an aspect ratio of 3.5. The dorsal edge of the paroccipital process bears a deep fossa that opens dorsally (Fig. 16), like that of *Tawa hallae* (GR 241), and this unique feature shared between the two taxa represents a synapomorphy (Appendix S1).

Only the ventral surface of the parabasisphenoid is visible (Fig. 3). The parabasisphenoid contribution of the basitubera appears similar to that of the contribution of the basioccipital: both contribute to a low swelling that is not well defined. The ventral surface of the parabasisphenoid is broad with a wide fossa occupying the surface, similar to that of *Tawa hallae* (GR 241). This differs from the much narrower homologous region in *Gnathovorax cabreirai* (CAPPA/UFSM 0009). The ventral surface of the parabasisphenoid bears a small foramen in the centre of the depression in *Ptychotherates bucculentus*, like that of *Tawa hallae* (GR 241).

The supraoccipital forms the medial edge of the posttemporal fenestrae (Figs 1, 3, 16). The dorsal peak of the supraoccipital is broad like that of *Tawa hallae* (GR 241) and not as laterally compressed as that of *Gnathovorax cabreirai* (CAPPA/UFSM 0009). Rugose, low ridges are present on the posterolateral side of the supraoccipital (Fig. 16). We cannot determine whether the supraoccipital forms the dorsal part of the foramen magnum.

Both stapes remain in articulation in the stapedial groove on the ventral surface of the paroccipital processes (Figs 3, 16). They are broken laterally and measure 1.5 mm in diameter. The footplates are not visible.

Hemimandible

Dentary. Parts of each element, 28 mm long on the right and *c.* 40 mm on the left, are preserved and compressed against one another medially, with the right being more exposed and easier to describe and study (Figs 1, 2, 17). The right fragment holds three teeth (referred to as d1–3 from mesial to distal) although the absolute tooth positions are unknown because of breakage. We cannot confirm whether interdental plates were present. Our reconstruction from CT data indicates that a concavity sits distal to tooth position d3, but it is bounded laterally by a displaced mass of bone and could represent damage rather than an alveolus. The ventral edge of both

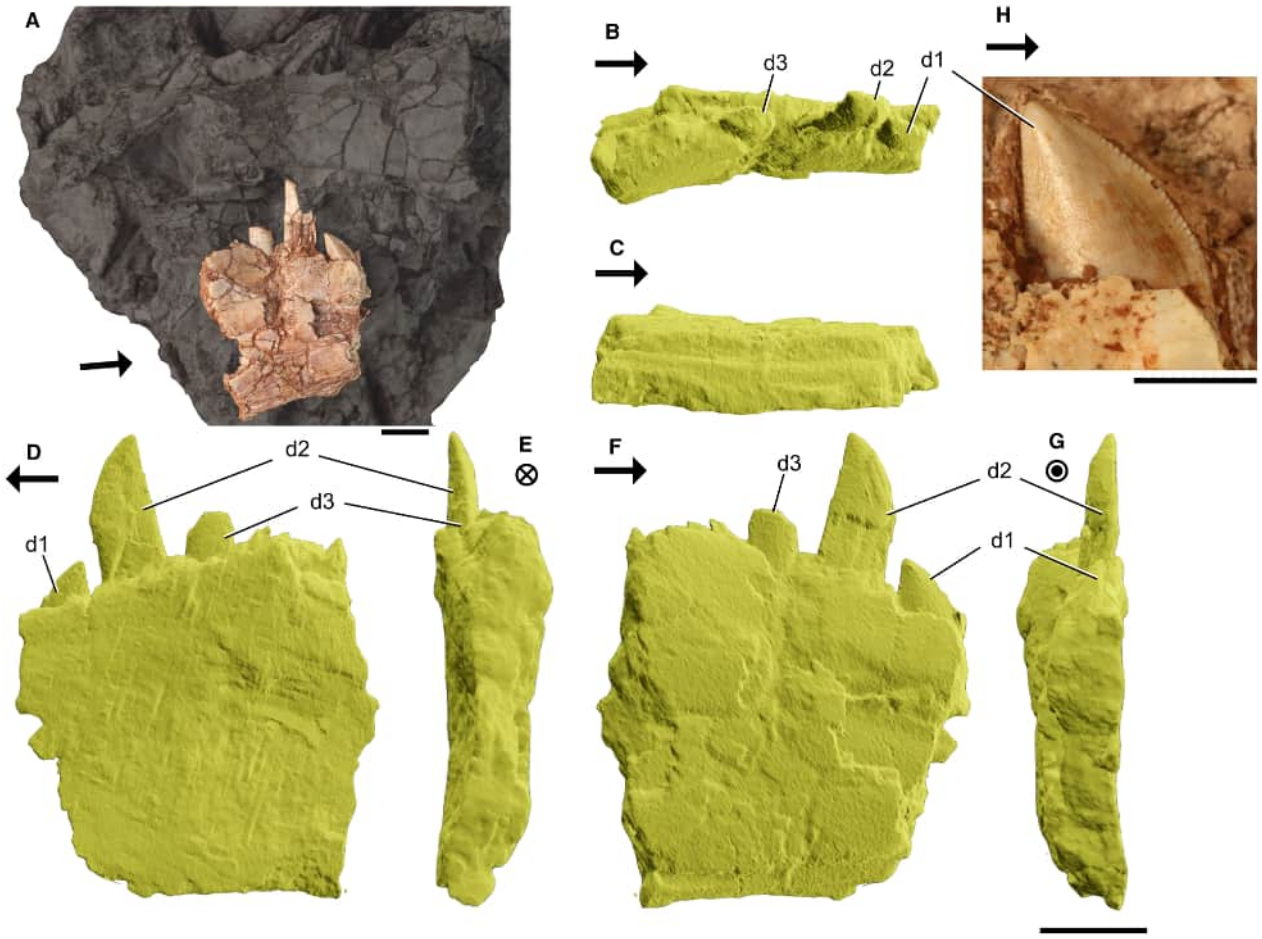

FIG. 17. The right dentary of *Ptychotherates bucculentus* (CM 31368). A, photograph of CM 31368 highlighting the right dentary in lateral view. B–G, digital reconstructions in: B, dorsal; C, ventral; D, medial; E, posterior; F, lateral; G, anterior view. H, photograph of the first preserved dentary tooth in labial view. *Abbreviations*: d1–3, preserved dentary tooth positions. Arrows indicate anterior direction, crossed circle indicates posterior out of page and dotted circle indicates anterior out of page. Scale bars represent: 1 cm (A, B–G); 5 mm (H).

dentaries appears nearly completely preserved but the right dentary bears a pair of longitudinal grooves from damage. The height of the preserved parts of the dentaries appears relatively deeper than in coelophysids (*Coelophysis bauri*, CM 31374) and possibly in the holotype of *Tawa hallae* (GR 241). The medial face lacks any trace of the Meckelian groove, owing either to the position of the preserved element or perhaps to obscuring by the splenial that we cannot distinguish from the dentary.

Postdentary bones. The postdentary bones that are preserved in *Ptychotherates bucculentus* include the left surangular, left articular and only the posterior portion of the prearticular (Figs 1, 2, 18). All of these elements remain in articulation with each other.

The left surangular of *Ptychotherates bucculentus* is laterally exposed and largely complete except for parts of the anterior and ventral edges (Fig. 18). The exposed section of the surangular is *c.* 9 cm long anteroposteriorly. The surangular forms the posterodorsal boundary of the external mandibular fenestra ('emf' in Figs 5, 18) and is preserved continuing anteriorly for a short distance past the left dentary, but could not be digitally reconstructed there reliably because of poor contrast.

In lateral view the dorsal edge of the surangular is dorsally convex immediately ventral to the left jugal. It appears to be more greatly convex than in *Tawa hallae* (GR 241) but this varies greatly between early dinosaurs, such as among neotheropods (e.g. *Dilophosaurus wetherilli*, UCMP 77270 has a more convex dorsal edge than *Zupaysaurus rougieri*, PULR-V 076) and early-diverging sauropodomorphs (e.g. *Eoraptor lunensis*, PVSJ 512 having a less convex dorsal edge than *Pampadromaeus barberenai*, ULBRA-PVT016). The anteroventral section of

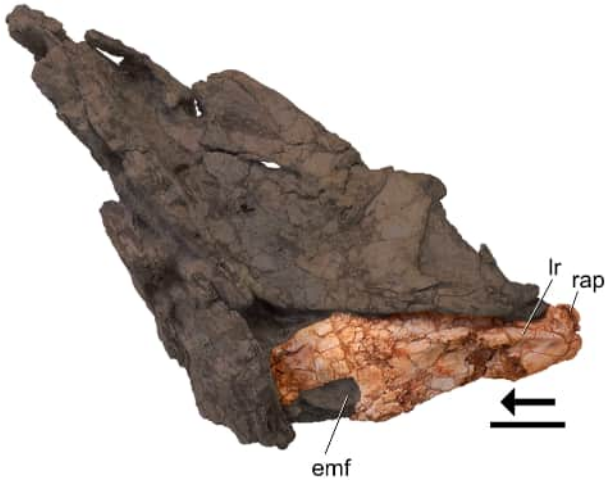

FIG. 18. Photograph of CM 31368 highlighting the left surangular and articular of *Ptychotherates bucculentus* in lateral view. *Abbreviations*: emf, external mandibular fenestra; lr, lateral ridge; rap, retroarticular process. Arrow indicates anterior direction. Scale bar represents 2 cm.

the surangular of *Ptychotherates bucculentus* is deeply excavated in lateral view by the posterodorsal border of the external mandibular fenestra (Fig. 18). The posterior corner of the fenestra is completely composed by the surangular because a portion of the surangular that bounded the fenestra ventrally is also preserved. This is similar to that of *Tawa hallae* (GR 241), *Gnathovorax cabreirai* (CAPPA/UFSM 0009) and the sauropodomorph *Pampadromaeus barberenai* (ULBRA-PVT016), but not to *Herrerasaurus ischigualastensis* (PVSJ 407), in which the posterior corner of the mandibular fenestra is composed ventrally by the angular.

The ventral edge of the surangular is incomplete, but the dorsoventral depth of the preserved section suggests an aspect ratio for the element that is clearly deeper than is known for *Tawa hallae* (GR 241, GR 1088). The deepest point of the surangular, immediately posterior to the external mandibular fenestra, is half of the anteroposterior length from the glenoid fossa to the external mandibular fenestra, compared with that of *Tawa hallae* (GR 241), which reaches only one-third (3 cm : 6 cm vs 1 cm : 3 cm).

The surangular is slightly laterally convex. The apex of this convexity is immediately posterior to the external mandibular fenestra, but the specimen is also cracked there, exaggerating the curvature. The ventral edge of the surangular is complete only in the articular region, ventral to the glenoid fossa, but it is still unclear whether the surangular would have abutted the angular for most of the ventral edge, as in *Coelophysis bauri* (CM 31374), or only anteriorly, as in '*Syntarsus*' *rhodesiensis* (Raath 1978). Laterally, there is clearly an anterior–posteriorly oriented lateral ridge ('lr' in Fig. 18) in *Ptychotherates bucculentus* similar to the surangular ridge in *Gnathovorax cabreirai* (CAPPA/UFSM 0009), *Tawa hallae* (GR 241), *Herrerasaurus ischigualastensis* (PVSJ 407) and neotheropods (*Coelophysis bauri*, Colbert 1989). It is not clear whether a surangular foramen is present on the lateral side of the surangular in *Ptychotherates bucculentus* because of breakage immediately ventral to the surangular ridge. The posterodorsal edge of the surangular is dorsally expanded like that of *Gnathovorax cabreirai* (CAPPA/UFSM 0009), *Tawa hallae* (GR 241) and *Herrerasaurus ischigualastensis* (PVSJ 407). The dorsal tip of the dorsal projection is broken but clearly shows a dorsal expansion, immediately posterior to the glenoid (referred to an expanded retroarticular process by some, see Phylogenetic characters). It is not clear whether the lateral side of the surangular formed any of the glenoid for articulation with the quadrate because of co-ossification between the surangular and articular.

The left articular is largely complete but obscured by the articulated quadrate. In dorsal view the articular expands medially to form a curve that is J shaped (Fig. 1). The retroarticular process ('rap' in Figs 16, 18) is not expanded posteriorly; the posterior edge of the glenoid of the articular is the posterior termination of the hemimandible. The anterior rim of the glenoid, as viewed medially, is taller than the posterior border of the glenoid. The entire medial surface of the articular is covered by the posterior end of the prearticular. The medial surface of the prearticular is smooth.

Dentition. There are many teeth of *Ptychotherates bucculentus* preserved *in situ* in CM 31368, but most are obscured by other skull elements or were damaged during fossilization or preparation (Figs 1, 2, 5, 6, 17). Only a few teeth are clearly exposed and close to their original shape: two from a position anteroposteriorly midway in the left maxilla in preserved positions 4 and 5 ('m4' and 'm5' in Fig. 6), and the first and second preserved teeth in the right dentary ('d1' and 'd2' in Fig. 17). More anteriorly positioned replacement teeth are visible in occlusal view of the fractured facial portion of the left maxilla (i.e. the first three maxillary tooth positions), but were difficult to digitally reconstruct because of poor contrast in the CT data. Much of the mesial carina of the third maxillary tooth is preserved and exposed (Fig. 6G), as is the crown base of the third dentary tooth (the apical half of the crown having left an impression on matrix lingual to it), but overall the dental sample is constrained to only those teeth from the middle of the tooth row. The distinction between the tooth root and alveolus was also unclear with the available CT data, therefore only the crowns can be described.

The tooth crowns of the preserved and exposed teeth of *Ptychotherates bucculentus* are triangular and taper to a single point, where the mesial edge is convex and the distal edge is straight (e.g. Fig. 17H). These teeth, like those positioned distally in *Tawa hallae* (GR 241), *Daemonosaurus chauliodus* (CM 76821) and *Coelophysis bauri* (CM 31368), lack the recurvature of a 'ziphodont' tooth as defined by Hendrickx *et al.* (2015) because their distal edges are not concave. The distal edge of each tooth of *Ptychotherates bucculentus* is apicobasally perpendicular to the mesiodistal axis, hence the crown apex is not distal to the distal extent of the alveolus. This contrasts with the teeth of *Herrerasaurus ischigualastensis* (PVSJ 407), in which the teeth throughout both the dentary and maxilla are fully recurved. Whereas the first and second preserved teeth in the right dentary of *Ptychotherates bucculentus* are 'lenticular' in cross-section *sensu* Hendrickx *et al.* (2015), the third appears 'lanceolate' (Fig. 17B).

The labial surfaces of the crowns of *Ptychotherates bucculentus* are smoothly convex, which differs from the apically basal grooves and ridges present in the holotype of *Tawa hallae* (GR 241). The mesial and distal carinae of *Ptychotherates bucculentus* are both finely serrated, bearing 4–5 min serrations per mm. The denticle shape is peculiar among coeval carnivorous dinosaurs in that, whereas the denticles of the distal carinae point directly distally, denticles on the mesial carinae have sharper external margins that are oriented slightly apically (Figs 6G, 17H). The mesial interdenticular diaphyses recurve basally. This denticle shape is identical to that of *Tawa hallae* (GR 241). It also strongly resembles those of *Buriolestes schultzi* (ULBRA-PVT 280, Cabreira *et al.* 2016, fig. 3; CAPPA/UFSM 0035, Müller *et al.* 2018, fig. 7) and *Daemonosaurus chauliodus* (CM 76821, Nesbitt & Sues 2021, fig. 7B), but the teeth of *Ptychotherates bucculentus* (CM 31368) feature an intermediate count of denticles per millimetre, more than *Buriolestes schultzi* and fewer than *Daemonosaurus chauliodus*. The denticle shape of *Ptychotherates bucculentus* is also similar to the distal denticles of *Troodon formosus* (DMNH 22837) as figured by Hendrickx *et al.* (2015, fig. 8H), but for *Ptychotherates bucculentus* they are equal to each other in size and are much smaller proportionally to the overall edge length.

RESULTS

Our analysis of the Ezcurra *et al.* (2023) dataset with our addition of *Ptychotherates bucculentus* and additional changes (Appendix S1) resulted in four most parsimonious trees (MPTs) of 1414 steps each (Fig. 19). Two character states identify *Ptychotherates bucculentus* as a dinosaur in this analysis: the separation of the exoccipitals at the floor of the endocranial cavity (78:1) and the presence of a supratemporal fossa (=frontoparietal fossa *sensu* Holliday *et al.* 2020) anterior to the supratemporal fenestra (90:1). Saurischia, including eusaurischians and herrerasaurians, is united by 19 characters, two of which are present in *Ptychotherates bucculentus* (presence of a parabasisphenoid recess, 69:1; ventral ramus of the opisthotic is not eclipsed in posterior view by the exoccipital, 76:0).

The monophyly of Herrerasauria (taxa more closely related to Herrerasauridae than to theropods, sauropodomorphs or ornithischians, *sensu* Garcia *et al.* 2024) is supported by 10 character states. Two of them, the lateral surface of the exoccipital lacking a subvertical crest (77:0) and the antorbital fossa not extending to the posterior ramus of the maxilla (87:0), were scored for *Ptychotherates bucculentus* and support the relationship within Herrerasauria. *Ptychotherates bucculentus* was scored differently for two character states that support Eusaurischia (a sharp ridge on the lateral surface of the maxilla (24:1) and an acute interior angle between the dorsal process and main axis of the jugal (321:1)), indicating that the new taxon falls outside of this clade.

Within Herrerasauria, a monophyletic Morphoraptora was consistently recovered containing *Chindesaurus bryansmalli*, *Tawa hallae*, *Ptychotherates bucculentus* and *Daemonosaurus chauliodus*. This clade was found as the sister taxon of Herrerasauridae, similarly to results of prior analyses (Ezcurra *et al.* 2023; Garcia *et al.* 2024). Two characters scoreable in *Ptychotherates bucculentus* are recovered as synapomorphies of this clade: the anterior extent of the jugal–quadratojugal joint bifurcation beyond the posterior edge of the dorsal jugal process (52:1), and the hatchet-like shape of the postorbital in dorsal view (382:2). A long anterior process of the quadratojugal (52:1) is found among neotheropods as well; in the scenario recovered here, this character state evolved independently in an ancestor of morphoraptorans and within Theropoda.

The relationships within this clade are not resolved in the strict consensus (Fig. 19), but inspection of each MPT shows that each recovered a closer relationship between *Tawa hallae* and *Ptychotherates bucculentus* than with either to *Daemonosaurus chauliodus*. The placement of *Chindesaurus bryansmalli* is either within an unresolved

FIG. 19. Strict consensus tree of four most parsimonious trees produced by a phylogenetic analysis of *Ptychotherates bucculentus* using a dataset derived from Ezcurra *et al.* (2023). Numbers above branches show Bremer support and '10+' indicates a Bremer support greater than 10; numbers below show GC frequencies from bootstrapping for groups recovered in that analysis.

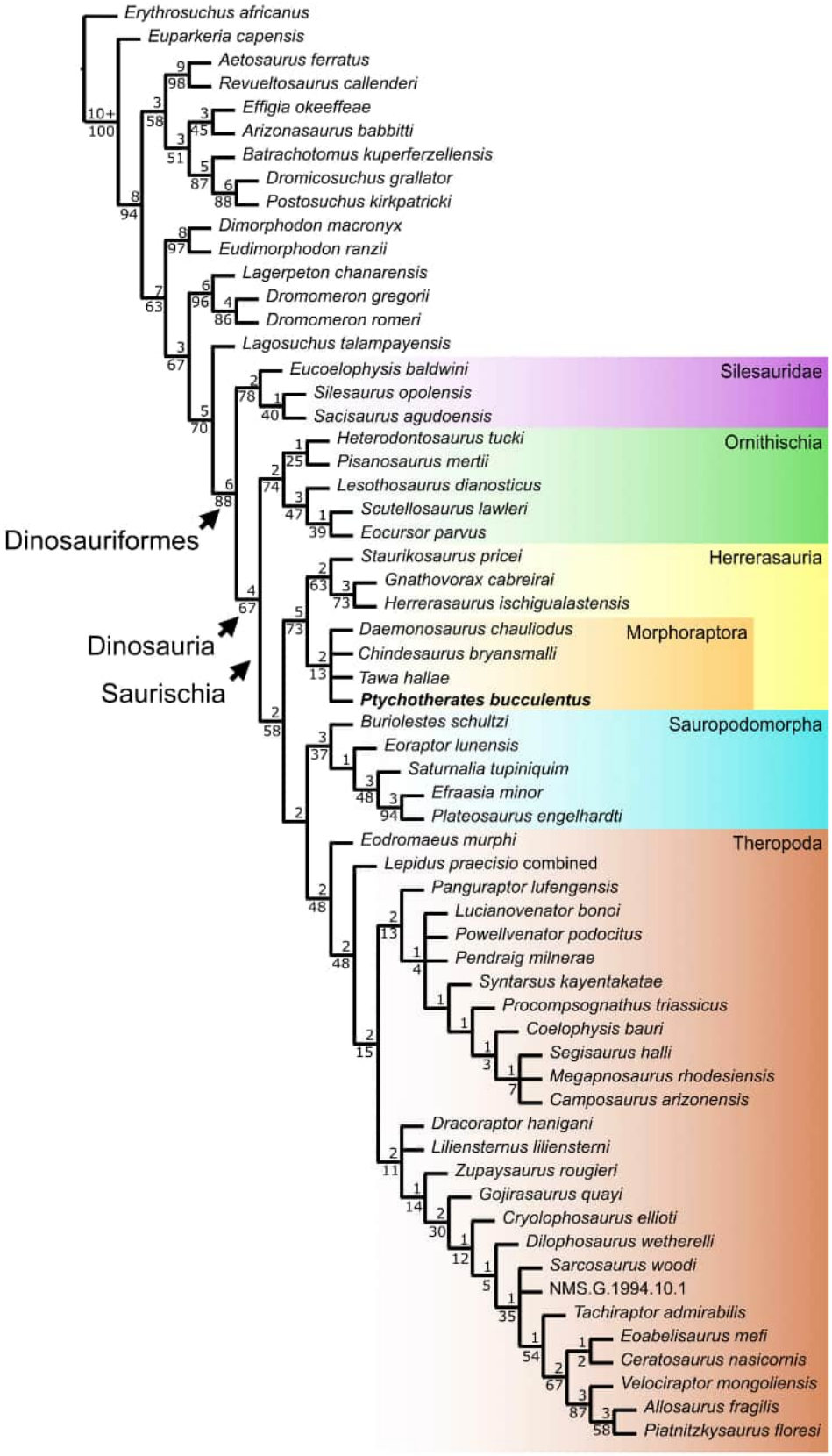
Erythrosuchus africanus
Euparkeria capensis
Aetosaurus ferratus
Revueltosaurus callenderi
Effigia okeeffeae
Arizonasaurus babbitti
Batrachotomus kuperferzellensis
Dromicosuchus grallator
Postosuchus kirkpatricki
Dimorphodon macronyx
Eudimorphodon ranzii
Lagerpeton chanarensis
Dromomeron gregorii
Dromomeron romeri
Lagosuchus talampayensis
Eucoelophysis baldwini
Silesaurus opolensis
Sacisaurus agudoensis
Silesauridae
Heterodontosaurus tucki
Pisanosaurus mertii
Lesothosaurus dianosticus
Scutellosaurus lawleri
Eocursor parvus
Ornithischia
Dinosauriformes
Staurikosaurus pricei
Gnathovorax cabreirai
Herrerasaurus ischigualastensis
Herrerasauria
Dinosauria
Daemonosaurus chauliodus
Chindesaurus bryansmalli
Tawa hallae
Ptychotherates bucculentus
Morphoraptora
Saurischia
Buriolestes schultzi
Eoraptor lunensis
Saturnalia tupiniquim
Efraasia minor
Plateosaurus engelhardti
Sauropodomorpha
Eodromaeus murphi
Lepidus praecisio combined
Panguraptor lufengensis
Lucianovenator bonoi
Powellvenator podocitus
Pendraig milnerae
Syntarsus kayentakatae
Procompsognathus triassicus
Coelophysis bauri
Segisaurus halli
Megapnosaurus rhodesiensis
Camposaurus arizonensis
Dracoraptor hanigani
Liliensternus liliensterni
Zupaysaurus rougieri
Gojirasaurus quayi
Cryolophosaurus ellioti
Dilophosaurus wetherelli
Sarcosaurus woodi
NMS.G.1994.10.1
Tachiraptor admirabilis
Eoabelisaurus mefi
Ceratosaurus nasicornis
Velociraptor mongoliensis
Allosaurus fragilis
Piatnitzkysaurus floresi
Theropoda

trichotomy with *Tawa hallae* and *Ptychotherates bucculentus*, or outside in a polytomy with *Daemonosaurus chauliodus*. This 'wildcard' placement of *Chindesaurus bryansmalli* is demonstrated by the construction of a strict consensus tree exclusive of *Chindesaurus bryansmalli* (after including it in the tree-searching analysis itself), which resolves *Tawa hallae* and *Ptychotherates bucculentus* as unambiguous sister taxa. The unresolved position of *Chindesaurus bryansmalli* is a consequence of the absence of any overlapping material, and hence character scores, between it and *Ptychotherates bucculentus*.

Ptychotherates bucculentus and *Tawa hallae* were, in every MPT, united exclusive of *Daemonosaurus chauliodus* by the absence of any longitudinal ridge on the lateral face of the jugal (57:0) and a jugal at least 30% as deep as the orbit height (383:1 or 2, ordered). The distribution of (57:0) is widespread among sampled dinosaurs, observed for the several ornithischians, neotheropods and the sauropodomorph *Plateosaurus trossingensis*; however, the presence of a sharp lateral ridge on the jugal (57:1) is resolved by this dataset as the plesiomorphic state for Dinosauria. Although the dorsoventral jugal heights of *Gnathovorax cabreirai* (CAPPA/UFSM 0009) and *Daemonosaurus chauliodus* (CM 76821) do not meet the threshold for character state 383:1, their jugals are yet more dorsoventrally tall than that of early-diverging eusaurischians such as *Coelophysis bauri* (CM 31374), *Panguraptor lufengensis* (LFGT-0103) and *Eoraptor lunensis* (PVSJ 512). This indicates that the ancestral herrerasaurian had a relatively deeper jugal than the ancestral eusaurischian, a trait for which *Ptychotherates bucculentus* presents a new extreme.

The two new characters we added (390 and 391) represent morphologies almost unique to *Tawa hallae* and *Ptychotherates bucculentus* (the posterior face of the quadrate possesses a deep, dorsoventrally oriented fossa, 390:1; the dorsal edge of the paroccipital process features a mediolaterally oriented groove, 391:1). Neither character state was found to be an unambiguous synapomorphy of *Tawa hallae* and *Ptychotherates bucculentus* with the inclusion of *Daemonosaurus chauliodus* and *Chindesaurus bryansmalli* in the dataset because these characters could not be scored in the latter two taxa. However, when *Daemonosaurus chauliodus* and *Chindesaurus bryansmalli* are removed from the dataset, both characters 390 and 391 optimize as synapomorphies of *Tawa hallae* and *Ptychotherates bucculentus*, demonstrating that the derived character states (i.e. 390:1; 391:1) are unique among early-diverging dinosaurs. However, it is not clear whether these two character states are found only in *Tawa hallae* and *Ptychotherates bucculentus* or also in other morphoraptorans.

Our analysis of the Griffin *et al.* (2022) dataset with our addition of *Ptychotherates bucculentus* and additional changes corroborated the findings of the dataset derived from Ezcurra *et al.* (2023) with respect to the close relationships of *Ptychotherates bucculentus*, although larger-scale relationships differed between the two datasets (Fig. 20A). Making only the listed alterations to the Griffin *et al.* (2022) data (Appendix S1) resulted in 6144 MPTs of 1957 steps. Herrerasauridae, most of the frequently recovered Sauropodomorpha (e.g. as recovered by Griffin *et al.* 2022) and a few theropod groups were recovered, but 20 genera were not resolved beyond a polytomy at the base of Dinosauria, including the morphoraptorans (i.e. *Ptychotherates bucculentus*, *Tawa hallae*, *Chindesaurus bryansmalli* and *Daemonosaurus chauliodus*) (Fig. 20A).

We observed in the MPTs themselves that, although relationships within previously established clades (e.g. Morphoraptora and Coelophysoidea) were stable, the unstable placement of taxa at the early-diverging positions of each clade produced uncertainty. In particular, we targeted and removed *Guaibasaurus candelariensis* from one analysis, which reduced the resulting trees to 288 MPTs, of 1946 steps each, that unanimously recovered clades in line with other analyses (Fig. 20B). The consensus of these MPTs conflicted with the dataset adapted from Ezcurra *et al.* (2023) in that Theropoda was sister to Ornithischia, and Herrerasauria was sister to Sauropodomorpha, but the analyses were in agreement regarding the more specific relationships of *Ptychotherates bucculentus* in that it was included in Morphoraptora, and that this clade was the sister taxon of Herrerasauridae.

According to the consensus of all MPTs of this dataset excluding *Guaibasaurus candelariensis*, *Ptychotherates bucculentus* can be diagnosed to Dinosauria only by the presence of the supratemporal fossa on the frontal (83:1). Five characters unite Sauropodomorpha and Herrerasauria (the latter including *Eodromaeus murphi* in these MPTs), and three unite *Eodromaeus murphi* with Herrerasauridae and Morphoraptora, but none of those characters was scored for *Ptychotherates bucculentus*. The synapomorphies shared by Herrerasauridae and Morphoraptora that are scoreable on *Ptychotherates bucculentus* are the absence of a lateral ridge on the maxilla (35:0) and the jugal being more than 20% as dorsoventrally deep as it is anteroposteriorly long anterior to the infratemporal fenestra (67:1). Morphoraptora was recovered with similar synapomorphies to the analyses performed with the Ezcurra *et al.* (2023) dataset: the extent of the posterior jugal bifurcation anteriorly beyond the infratemporal fenestra (61:1) and the distinct hatchet-like shape of the postorbital in dorsal view (69:2). The lateral overlap of the lacrimal over the jugal (66:0) was recovered as an autapomorphy of *Ptychotherates bucculentus*, but this character is difficult to reconstruct and scored variably, possibly calling for revision.

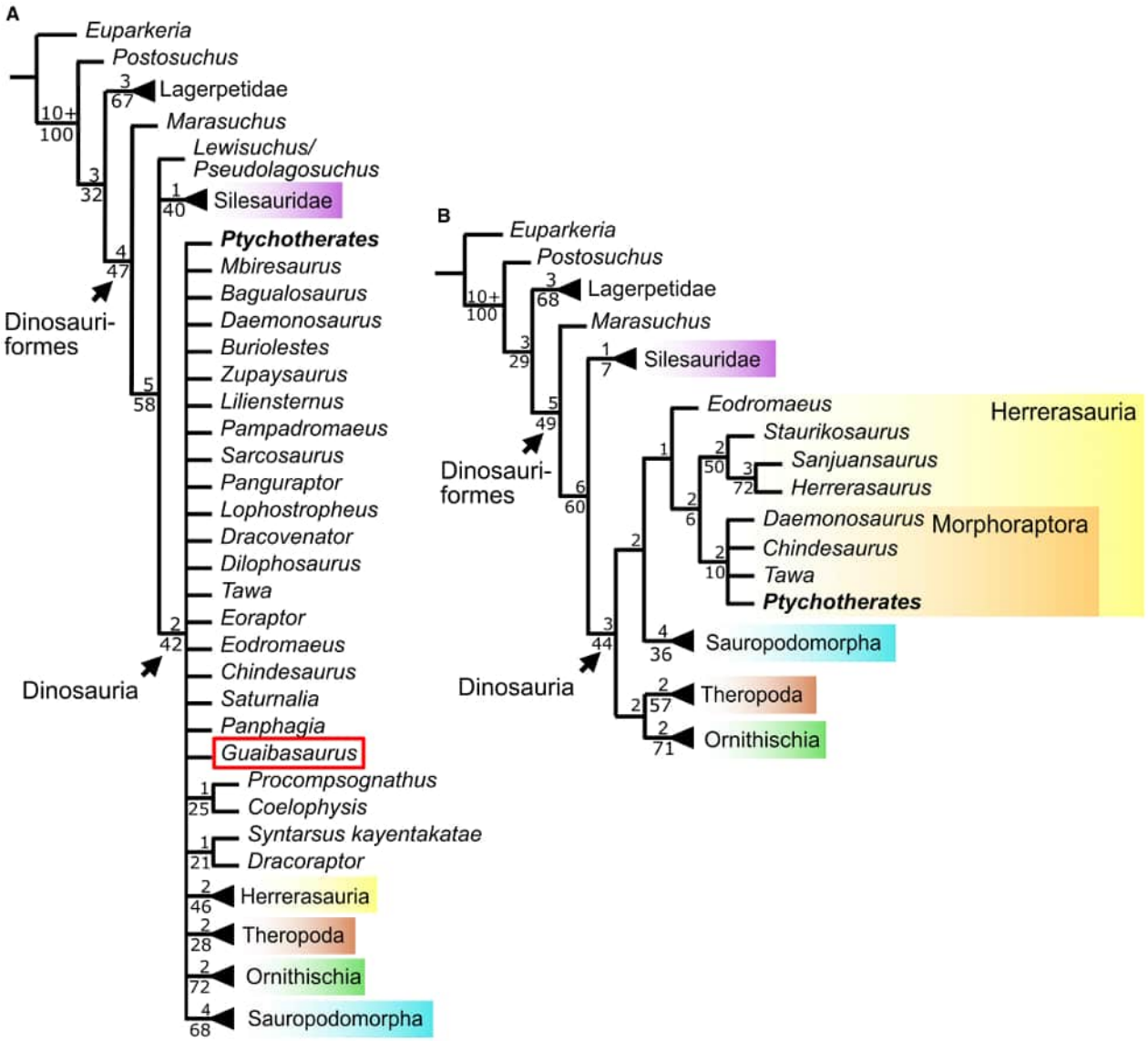

FIG. 20. Simplified strict consensus trees of most parsimonious trees produced by phylogenetic analyses of *Ptychotherates bucculentus* using a dataset derived from Griffin *et al.* (2022). A, strict consensus of 6144 most parsimonious trees after making only the character and score modifications outlined in Appendix S1 in addition to scoring *Ptychotherates bucculentus*. B, strict consensus of 288 most parsimonious trees after removing *Guaibasaurus candelariensis* (boxed in red; justification in Results section) in addition to the data used for tree A. Numbers above branches show Bremer support and '10+' indicates a Bremer support greater than 10; numbers below show GC frequencies from bootstrapping for groups recovered in that analysis. Complete trees available in Appendix S1.

Just as with the former phylogenetic analysis, although *Daemonosaurus chauliodus* appears under strict consensus to nest with the core Morphoraptora, the removal of *Chindesaurus bryansmalli* after analysis produces an unambiguous sister-taxon relationship between *Tawa hallae* and *Ptychotherates bucculentus*. Without additional taxon deletions from the data used for tree searching, the only unambiguous synapomorphy of *Ptychotherates bucculentus* and *Tawa hallae* is the lack of a longitudinal ridge on the lateral face of the jugal (58:0). We performed additional analyses on datasets by deleting the problematic *Guaibasaurus candelariensis*, *Chindesaurus bryansmalli* and *Daemonosaurus chauliodus* to see what character states were optimized as synapomorphies between *Ptychotherates bucculentus* and *Tawa hallae*. The character state support list expanded to include the paroccipital process extending laterally rather than ventrally (86:0), the exoccipital lacking a vertical crest (=metotic strut) (92:0), and a prominent and dorsally deflected retroarticular process being present (145:0). In addition

to the two characters added in this study (458 and 459), the presence of a dorsoventrally oriented fossa on the posterior face of the quadrate (458:1) and a groove on the dorsal edge of the paroccipital process (459:1) optimized as synapomorphies of *Ptychotherates bucculentus* and *Tawa hallae*, as in the results of the Ezcurra *et al.* (2023) dataset.

DISCUSSION

Emergence of Morphoraptora

Through anatomical comparison with other Triassic archosaurs and inclusion in phylogenetic analyses, we support *Ptychotherates bucculentus* as a new taxon of saurischian dinosaur closely related to *Tawa hallae*. More broadly, we recover *Ptychotherates bucculentus* as a member of Morphoraptora, a clade known exclusively from the Upper Triassic deposits of southwestern USA. At the core of Morphoraptora, the polytomy of *Ptychotherates bucculentus*, *Tawa hallae*, *Chindesaurus bryansmalli* and *Daemonosaurus chauliodus* is currently unresolvable partially because of the lack of overlap between the holotypes of *Chindesaurus bryansmalli* (a postcranial skeleton; PEFO 10395), *Daemonosaurus chauliodus* (a skull and some of the neck; CM 76821) and *Ptychotherates bucculentus* (a skull; CM 31368). Nevertheless, the nearly complete holotype skeleton (GR 241) of *Tawa hallae* (Nesbitt *et al.* 2009) serves to unite these four taxa by indicating the shared derivation of both cranial and postcranial apomorphies.

For the first time, we found *Daemonosaurus chauliodus* within Morphoraptora; previously, *Daemonosaurus chauliodus* has been found at a similar phylogenetic position to Morphoraptora (Sues *et al.* 2011; Nesbitt & Sues 2021), but never closer to this clade than to other lineages. Comparatively, *Daemonosaurus chauliodus* has an anteroposteriorly short snout and dorsoventrally tall premaxilla bearing procumbent teeth (Sues *et al.* 2011; Nesbitt & Sues 2021) whereas *Tawa hallae* has a proportionally longer snout and premaxilla (Nesbitt *et al.* 2009). Thus, the recognition of a fourth member *Ptychotherates bucculentus* with an exceptionally dorsoventrally tall jugal points to undiscovered cranial disparity among the herrerasaurians.

Ptychotherates bucculentus represents a clear member of Morphoraptora, which was found as sister to Herrerasauridae within Herrerasauria outside of Sauropodomorpha, Theropoda and Ornithischia (Figs 19, 20). The inclusion of Morphoraptora within Herrerasauria is rather well supported, but we do note that small changes in character scores and taxon and character inclusion in similar analyses find positions for the clade immediately outside Eusaurischia and less closely related to Herrerasauridae (Marsh *et al.* 2019; Nesbitt & Sues 2021), or possibly within Theropoda (Nesbitt *et al.* 2009; Martinez *et al.* 2011). Like *Tawa hallae*, the skull of *Ptychotherates bucculentus* bears a mosaic of derived herrerasaurian and neotheropod attributes (Cabreira *et al.* 2016; Baron *et al.* 2017b; Marsh *et al.* 2019; Nesbitt & Sues 2021). *Ptychotherates bucculentus* does not help resolve the contentious phylogenetic position of the morphoraptorans among early-diverging dinosaurs, nor the interrelationships between other large clades.

The longevity and diversity of Morphoraptora

Ptychotherates bucculentus is from the *Coelophysis* Quarry, a locality that is inferred to be Rhaetian or latest Norian in age through multiple independent lines of evidence including biostratigraphy, lithostratigraphy and magnetochronology (see above). Because *Daemonosaurus chauliodus* is also from the same locality, they are equally the youngest-occurring herrerasaurians. Inferring that *Daemonosaurus chauliodus* is a morphoraptoran would have indicated the longevity of the clade more than a decade ago (and was explored by Novas *et al.* 2021), but many aspects of the morphology of *Daemonosaurus chauliodus* are so aberrant from any other established dinosaur clade that its closer association with morphoraptorans than other dinosaurs hinges on only a few synapomorphies (Nesbitt & Sues 2021). Although we find evidence for the placement of *Daemonosaurus chauliodus* as a herrerasaurian, the closer affinities of *Ptychotherates bucculentus* to *Tawa hallae* are a clearer record of the longevity of the clade throughout the deposition of the Chinle Formation.

Other morphoraptorans occur in the same stratigraphic sequence in the same geographic region (i.e. Chama Basin) but in another, lower member of the Chinle Formation (i.e. *Tawa hallae* from the Petrified Forest Member of the Chinle Formation at Ghost Ranch) and in correlated sediments that are older and which occur in other geographic regions (*Chindesaurus bryansmalli* from the Petrified Forest Member in Arizona). Furthermore, isolated bones and partial skeletons diagnostic of Morphoraptora are present across southwestern USA in Upper Triassic sediments. These include further remains from the Chinle Formation of Arizona (Marsh & Parker 2020) and from the Dockum Group of Texas (Long & Murry 1995; Nesbitt & Chatterjee 2008; Sarıgül 2017; Marsh & Parker 2020), possibly including the oldest sediment from the Dockum Group, the Otis Chalk Quarries (Long & Murry 1995; Stocker 2013). Thus, the clade appears widespread through time and space during the Late Triassic in southwestern USA. Moreover, the uppermost Triassic occurrence of *Ptychotherates bucculentus* and

Daemonosaurus chauliodus in the *Coelophysis* Quarry implies that the clade survived to near the end of the Triassic. The recovery of specimens in other uppermost Triassic strata such as the Nugget sandstone of Utah would support this scenario.

Throughout the Late Triassic, the dinosaur assemblages in southwestern USA consisted of at least one member of Herrerasauria and at least a member of Neotheropoda for nearly the entire length of the deposition of the Chinle Formation and the Dockum Group. At the same time, sauropodomorphs and unambiguous ornithischians were absent in the same assemblages (Nesbitt *et al.* 2007; Whiteside *et al.* 2015, but see Lovelace *et al.* 2025 for a different possibility for the earliest Late Triassic). Toward the end of the Triassic, this composition of dinosaur assemblages was maintained, and more than one herrerasaurian was present as evidenced by the *Coelophysis* Quarry. In the succeeding Early Jurassic, dinosaur assemblages in this area saw the introduction of herbivorous sauropodomorphs (e.g. *Sarahsaurus aurifontanalis*, Rowe *et al.* 2011; Marsh & Rowe 2018) and ornithischians (*Scutellosaurus lawleri*, Colbert 1981; *Scelidosaurus*, Padian 1989; Heterodontosauridae, DeVries & Sereno 2024). Among the carnivorous clades, whereas neotheropod lineages remained (e.g. '*Syntarsus*' *kayentakatae* Rowe 1989; *Dilophosaurus wetherilli*, Welles 1954; Marsh & Rowe 2020), morphoraptorans are absent, their extermination conspicuously occurring in the same window of time as the End-Triassic Extinction Event.

The lowest stages of the Jurassic Period are lacking in the stratigraphic record of Southwestern USA, and no localities in the area can confidently be assessed as terminal Triassic, blurring the line for how the End-Triassic Extinction Event affected diversity at the level of a smaller clade such as Morphoraptora. Nevertheless, Jurassic-aged localities worldwide lack any herrerasaurians, and we find here that Morphoraptora was represented by at least two distinct species very late into the Triassic. We predict that future discoveries will strengthen this pattern, and the view that Morphoraptora, and by extension Herrerasauria as a whole, went extinct at the End-Triassic Extinction Event. In this scenario, the End-Triassic Extinction Event would be more devastating for dinosaur diversity than previously recognized (e.g. Olsen *et al.* 2022).

Implications for Late Triassic dinosaur distribution across Pangaea

Many recent studies (Whiteside *et al.* 2015; Griffin *et al.* 2022; Dunne *et al.* 2023; Heath *et al.* 2025) explored dinosaur diversity in the Triassic and its relationships with geographic distribution across Pangea. Specific studies targeting carnivorous dinosaurs have shown a clear difference in diversity in the early phases of dinosaurian evolution: in the Carnian, the oldest-occurring carnivorous dinosaurs are well represented from higher-latitude Pangaea in current-day Argentina (Novas *et al.* 2021; Langer *et al.* 2022), Brazil (Novas *et al.* 2021; Langer *et al.* 2022; Garcia *et al.* 2021, 2024), Zimbabwe (Griffin *et al.* 2022) and India (Novas *et al.* 2010). In contrast, overlying Norian beds in the same region are nearly devoid of carnivorous saurischians outside of Neotheropoda (Novas *et al.* 2021), except in the early part of the Norian in modern India (Novas *et al.* 2010, Ezcurra *et al.* 2025). The Norian localities in Poland (Niedźwiedzki *et al.* 2014; Mujal *et al.* 2025) and throughout the Upper Triassic deposits of southwestern USA (Sues *et al.* 2011; Marsh & Parker 2020) do bear early-diverging carnivorous saurischians, but the more fragmentary record of non-neotheropod carnivorous dinosaurs has typically obstructed their clear assignment to any clade, and thus precludes recognition of patterns of diversity of those clades later in the Triassic.

The recognition of a second late surviving morphoraptoran, *Ptychotherates bucculentus*, demonstrates the longevity of a carnivorous early-diverging dinosaur clade in low latitudes for most of the Late Triassic of Pangaea (Kent & Irving 2010). The phylogenetic position of Morphoraptora within Herrerasauria implies an early divergence with other dinosaurian groups within the Carnian at or near the origin of dinosaurs *c.* 233 Ma (Langer *et al.* 2018). This observation is largely still consistent with the alternative phylogenetic positions of morphoraptorans within Theropoda found by others (e.g. Nesbitt *et al.* 2009; Martinez *et al.* 2011) given the appearance of more theropod-like taxa such as *Eodromaeus murphi* in some of the same early dinosaur deposits in Argentina (Martinez *et al.* 2011). Furthermore, the absence of clear morphoraptorans outside of the low latitudes for tens of millions of years implies that this group may have been endemic to environmental conditions present in the low latitudes for the Late Triassic (Fig. 4D). However, some potential remains of herrerasaurians and other adjacent saurischians have been found outside the region from the lower Norian of India (Ezcurra *et al.* 2025) and even the upper Norian of Poland (Niedźwiedzki *et al.* 2014).

Nevertheless, the herrerasaurians of the *Coelophysis* Quarry are the latest-occurring worldwide and are potentially the only known Rhaetian herrerasaurians. This hints at the possibility that the low latitudes may have represented a 'museum' (Stebbins 1974; Vasconcelos *et al.* 2022) with regards to early-diverging carnivorous dinosaurs. Furthermore, the 'museum' in the low latitudes seems to have prevented invasion of later Triassic dinosaurs, such as sauropodomorphs (Whiteside *et al.* 2015), which were thriving in the higher latitudes of both the northern and southern parts of Pangea. More fossils from

similarly aged deposits across Pangea will help us to refine the chronology of how herrerasaurians evolved and died out at various latitudes, but the discovery and identification of *Ptychotherates bucculentus* underlines the notion that Herrerasauria contributed to dinosaurian diversity in the low latitudes for nearly the entire Late Triassic.

CONCLUSION

Ptychotherates bucculentus is a newly described species of non-neotheropod carnivorous dinosaur from the uppermost Triassic *Coelophysis* Quarry in northern New Mexico, represented by a nearly complete skull. Our phylogenetic analyses align *Ptychotherates bucculentus* with *Tawa hallae*, *Chindesaurus bryansmalli* and *Daemonosaurus chauliodus* in a clade Morphoraptora closely related to Herrerasauridae, and outside Theropoda and Sauropodomorpha. The holotypes of *Ptychotherates bucculentus*, *Tawa hallae* and *Chindesaurus bryansmalli* do not overlap anatomically sufficiently to resolve intra-clade relationships, but the presence of the lineage in the *Coelophysis* Quarry establishes that neotheropods coexisted with a clade of non-neotheropod carnivorous dinosaurs in low-latitude Pangea for much of the Late Triassic. The occurrence of morphoraptorans in the *Coelophysis* Quarry assemblage extends their stratigraphic range later in the Triassic than previously thought, and the extinction of Morphoraptora in the fossil record now appears much closer to the End-Triassic Mass Extinction. Whereas higher-palaeolatitude Pangea in the Rhaetian was lacking in morphoraptorans or other herrerasaurians, these dinosaurs persisted in equatorial Pangea and contributed to a distinct low-latitude Late Triassic dinosaur assemblage in the absence of sauropodomorphs and ornithischians.

Acknowledgements. We thank Amy Henrici and Matthew Lamanna for loaning the specimen. We thank Alex Downs, Vicki Yarborough and Annamarie Fadorsen for skilful preparation of the specimen. Justin Gladman provided critical assistance for acquiring a CT scan of the specimen at Duke University (SMiF). We thank Michelle Stocker for the use of computers and programs for CT segmentation. Discussions with Michelle Stocker, Randall Irmis, Matthew Carrano, David Berman, Hans-Dieter Sues, Eudald Mujal, Ben Kligman and Adam Fitch were important for completion of the description and interpretation of the early evolution of dinosaurs with this new specimen. The Virginia Tech paleobiology research group (Erika Goldsmith, Jack Stack, Emily Keeble, Isaac Pugh, Helen Burch) is thanked for their feedback and their support. Reviews from Adam Marsh, Martín Ezcurra, and an anonymous reviewer strengthened and sharpened this study and the manuscript. Executing and presenting this research required crucial support from the National Science Foundation (NSF EAR 1943286, NSF EAR 1349667), Barry Goldwater Scholarship and Excellence in Education Foundation, Fralin Life Sciences Institute and Virginia Tech Office of Undergraduate Research.

Author contributions. **Conceptualization** Simba Srivastava (SS), Sterling James Nesbitt (SJN); **Data Curation** SS, SJN; **Formal Analysis** SS, SJN; **Investigation** SS, SJN; **Methodology** SS, SJN; **Resources** SJN; **Visualization** SS, SJN; **Writing – Original Draft Preparation** SS, SJN; **Writing – Review and Editing** SS, SJN.

DATA ARCHIVING STATEMENT

Data for this study are available in the MorphoSource digital repository: https://www.morphosource.org/projects/000794729; individual DOIs are listed in Table S1.

This published work, and the nomenclatural acts it contains, have been registered in ZooBank: https://zoobank.org/References/3bf4f754-ed0c-4c40-be91-f91538252687

Editor. Paul Barrett

SUPPORTING INFORMATION

Additional Supporting Information can be found online (https://doi.org/10.1002/spp2.70069):

Appendix S1. Phylogenetic dataset modifications and scoring for *Ptychotherates bucculentus*; complete consensus trees.
Appendix S2. Nexus files.
Table S1. MorphoSource DOIs associated with this publication.

REFERENCES

Baron, M. G., Norman, D. B. and Barrett, P. M. 2017a. A new hypothesis of dinosaur relationships and early dinosaur evolution. *Nature*, **543**, 501–506.

Baron, M. G., Norman, D. B. and Barrett, P. M. 2017b. Baron *et al.* reply. *Nature*, **551**, E4–E5.

Bonaparte, J. F. and Powell, J. E. 1980. A continental assemblage of tetrapods from the Upper Cretaceous beds of El Brete, northwestern Argentina (Sauropoda-Coelurosauria-Carnosauria-Aves). *Mémoires la Société Géologique de France*, **139**, 19–28.

Brusatte, S. L., Nesbitt, S. J., Irmis, R. B., Butler, R. J., Benton, M. J. and Norell, M. A. 2010. The origin and early radiation of dinosaurs. *Earth-Science Reviews*, **101**, 68–100.

Cabreira, S. F., Kellner, A. W. A., Dias-Da-Silva, S., Da Silva, L. R., Bronzati, M., De Almeida Marsola, J. C., Müller, R. T., De Souza Bittencourt, J., Batista, B. J. A. and Raugust, T. 2016. A unique Late Triassic dinosauromorph assemblage reveals dinosaur ancestral anatomy and diet. *Current Biology*, **26**, 3090–3095.

Clark, J. M., Sues, H.-D. and Berman, D. S. 2001. A new specimen of *Hesperosuchus agilis* from the Upper Triassic of New

Mexico and the interrelationships of basal crocodylomorph archosaurs. *Journal of Vertebrate Paleontology*, **20**, 683–704.

Colbert, E. H. 1981. A primitive ornithischian dinosaur from the Kayenta Formation of Arizona. *Museum of Northern Arizona Bulletin*, **53**, 1–61.

Colbert, E. H. 1989. *The Triassic dinosaur* Coelophysis. *Museum of Northern Arizona, Bulletin*, **57**, 1–160.

DeVries, R. P. and Sereno, P. C. 2024. Tiny dinosaur from the Kayenta Formation (Early Jurassic: Pliensbachian) of northern Arizona implicates dwarfing and insectivory at the base of the heterodontosaurid radiation. *Journal of Vertebrate Palaeontology*, Program and Abstracts **2024**, 174–175.

Dunne, E. M., Farnsworth, A., Benson, R. B., Godoy, P. L., Greene, S. E., Valdes, P. J., Lunt, D. J. and Butler, R. J. 2023. Climatic controls on the ecological ascendancy of dinosaurs. *Current Biology*, **33**, 206–214.

Dzik, J. 2003. A beaked herbivorous archosaur with dinosaur affinities from the early Late Triassic of Poland. *Journal of Vertebrate Paleontology*, **23**, 556–574.

Ezcurra, M. D. 2007. The cranial anatomy of the coelophysoid theropod *Zupaysaurus rougieri* from the Upper Triassic of Argentina. *Historical Biology*, **19**, 185–202.

Ezcurra, M. D. 2012. Comments on the taxonomic diversity and paleobiogeography of the earliest known dinosaur assemblages (late Carnian–earliest Norian). *Historia Natural*, **2**, 49–71.

Ezcurra, M. D., Garcia, M. S., Novas, F. E., Müller, R. T., Agnolín, F. L. and Chatterjee, S. 2025. A new herrerasaurian dinosaur from the Upper Triassic Upper Maleri Formation of south-central India. *Royal Society Open Science*, **12**, 250081.

Ezcurra, M. D., Marke, D., Walsh, S. A. and Brusatte, S. L. 2023. A revision of the 'coelophysoid-grade' theropod specimen from the Lower Jurassic of the Isle of Skye (Scotland). *Scottish Journal of Geology*, **59**, sjg2023-012.

Fitch, A., Lovelace, D. and Stocker, M. R. 2020. The oldest dinosaur from the northern hemisphere and the origins of Theropoda. *Journal of Vertebrate Palaeontology*, Program and Abstracts **2020**, 140–141.

Garcia, M. S., Cabreira, S. F., Da Silva, L. R., Pretto, F. A. and Müller, R. T. 2024. A saurischian (Archosauria, Dinosauria) ilium from the Upper Triassic of southern Brazil and the rise of Herrerasauria. *The Anatomical Record*, **307**, 1011–1024.

Garcia, M. S., Müller, R. T., Pretto, F. A., Da-Rosa, Á. A. and Dias-Da-Silva, S. 2021. Taxonomic and phylogenetic reassessment of a large-bodied dinosaur from the earliest dinosaur-bearing beds (Carnian, Upper Triassic) from southern Brazil. *Journal of Systematic Palaeontology*, **19**, 1–37.

Gauthier, J., Langer, M., Bittencourt, J., Novas, F. and Ezcurra, M. 2020. Saurischia. 1219–1224. *In* de Queiroz, K., Cantino, P. D. and Gauthier, J. A. (eds) *Phylonyms: A companion to the PhyloCode*. CRC Press.

Goloboff, P. A. and Morales, M. E. 2023. TNT version 1.6, with a graphical interface for MacOS and Linux, including new routines in parallel. *Cladistics*, **39**, 144–153.

Griffin, C. T., Stocker, M. R., Colleary, C., Stefanic, C. M., Lessner, E. J., Riegler, M., Formoso, K., Koeller, K. and Nesbitt, S. J. 2021. Assessing ontogenetic maturity in extinct saurian reptiles. *Biological Reviews*, **96**, 470–525.

Griffin, C. T., Wynd, B. M., Munyikwa, D., Broderick, T. J., Zondo, M., Tolan, S., Langer, M. C., Nesbitt, S. J. and Taruvinga, H. R. 2022. Africa's oldest dinosaurs reveal early suppression of dinosaur distribution. *Nature*, **609**, 313–319.

Heath, J. A., Cooper, N., Upchurch, P. and Mannion, P. D. 2025. Accounting for sampling heterogeneity suggests a low paleolatitude origin for dinosaurs. *Current Biology*, **35**, 941–953.

Hendrickx, C., Mateus, O. and Araújo, R. 2015. A proposed terminology of theropod teeth (Dinosauria, Saurischia). *Journal of Vertebrate Paleontology*, **35**, e982797.

Holliday, C. M., Porter, W. R., Vliet, K. A. and Witmer, L. M. 2020. The frontoparietal fossa and dorsotemporal fenestra of archosaurs and their significance for interpretations of vascular and muscular anatomy in dinosaurs. *The Anatomical Record*, **303**, 1060–1074.

Irmis, R. B., Mundil, R., Martz, J. W. and Parker, W. G. 2011. High-resolution U–Pb ages from the Upper Triassic Chinle Formation (New Mexico, USA) support a diachronous rise of dinosaurs. *Earth and Planetary Science Letters*, **309**, 258–267.

Irmis, R. B., Nesbitt, S. J., Padian, K., Smith, N. D., Turner, A. H., Woody, D. and Downs, A. 2007. A Late Triassic dinosauromorph assemblage from New Mexico and the rise of dinosaurs. *Science*, **317**, 358–361.

Kent, D. V. and Irving, E. 2010. Influence of inclination error in sedimentary rocks on the Triassic and Jurassic apparent pole wander path for North America and implications for Cordilleran tectonics. *Journal of Geophysical Research: Solid Earth*, **115**, B10103.

Kent, D. V., Olsen, P. E., Lepre, C., Rasmussen, C., Mundil, R., Gehrels, G. E., Giesler, D., Irmis, R. B., Geissman, J. W. and Parker, W. G. 2019. Magnetochronology of the entire Chinle Formation (Norian age) in a scientific drill core from Petrified Forest National Park (Arizona, USA) and implications for regional and global correlations in the Late Triassic. *Geochemistry, Geophysics, Geosystems*, **20**, 4654–4664.

Langer, M. C. and Benton, M. J. 2006. Early dinosaurs: a phylogenetic study. *Journal of Systematic Palaeontology*, **4**, 309–358.

Langer, M. C., Ezcurra, M. D., Bittencourt, J. S. and Novas, F. E. 2010. The origin and early evolution of dinosaurs. *Biological Reviews*, **85**, 55–110.

Langer, M. C., Ezcurra, M. D., Rauhut, O. W., Benton, M. J., Knoll, F., McPhee, B. W., Novas, F. E., Pol, D. and Brusatte, S. L. 2017. Untangling the dinosaur family tree. *Nature*, **551**, E1–E3.

Langer, M. C., McPhee, B. W., Marsola, J. C. D. A., Roberto-Da-Silva, L. and Cabreira, S. F. 2019. Anatomy of the dinosaur *Pampadromaeus barberenai* (Saurischia–Sauropodomorpha) from the Late Triassic Santa Maria Formation of southern Brazil. *PLoS One*, **14**, e0212543.

Langer, M., Novas, F. E., Bittencourt, J., Ezcurra, M. D. and Gauthier, J. A. 2020. Dinosauria R. Owen 1842. 1209–1217. *In* de Queiroz, K., Cantino, P. D. and Gauthier, J. A. (eds) *Phylonyms: A companion to the PhyloCode*. CRC Press.

Langer, M. C., Marsola, J. C., Müller, R. T., Bronzati, M., Bittencourt, J. S., Apaldetti, C. and Ezcurra, M. D. 2022. The early radiation of sauropodomorphs in the Carnian (Late

Triassic) of South America. 1–49. *In* Otero, A., Carballido, J. L. and Pol, D. (eds) *South American sauropodomorph dinosaurs: Record, diversity and evolution*. Springer.

Langer, M. C., Ramezani, J. and Da Rosa, Á. A. 2018. U-Pb age constraints on dinosaur rise from south Brazil. *Gondwana Research*, **57**, 133–140.

Linnaeus, C. 1758. *Systema naturae per regna tria naturae, secundum classes, ordines, genera, species, cum characteribus, differentiis, synonymis, locis. Tomus I. Editio decima, reformata*. Laurentius Salvius, Stockholm, 824 pp.

Long, R. A. and Murry, P. A. 1995. *Late Triassic (Carnian and Norian) tetrapods from the southwestern United States*. New Mexico Museum of Natural History and Science, Bulletin 4.

Lovelace, D. M., Kufner, A. M., Fitch, A. J., Curry Rogers, K., Schmitz, M., Schwartz, D. M., Leclair-Diaz, A., St. Clair, L., Mann, J. and Teran, R. 2025. Rethinking dinosaur origins: oldest known equatorial dinosaur-bearing assemblage (mid-late Carnian Popo Agie Fm, Wyoming, USA). *Zoological Journal of the Linnean Society*, **203**, zlae153.

Lucas, S. G. 1998. Global Triassic tetrapod biostratigraphy and biochronology. *Palaeogeography, Palaeoclimatology, Palaeoecology*, **143**, 347–384.

Lucas, S. G., Zeigler, K. E., Heckert, A. B. and Hunt, A. P. 2005. Review of Upper Triassic stratigraphy and biostratigraphy in the Chama Basin, northern New Mexico. Geology of the Chama Basin, 56th Field Conference. New Mexico Geological Society, 170–181.

Madsen, J. H. Jr 1976. *Allosaurus fragilis: A revised osteology*. Utah Geological and Mineral Survey, Bulletin 109.

Marsh, A. D. and Parker, W. G. 2020. New dinosauromorph specimens from Petrified Forest National Park and a global biostratigraphic review of Triassic dinosauromorph body fossils. *PaleoBios*, **37**, 1–56.

Marsh, A. D., Parker, W. G., Langer, M. C. and Nesbitt, S. J. 2019. Redescription of the holotype specimen of *Chindesaurus bryansmalli* Long and Murry, 1995 (Dinosauria, Theropoda), from Petrified Forest National Park, Arizona. *Journal of Vertebrate Paleontology*, **39**, e1645682.

Marsh, A. D. and Rowe, T. B. 2018. Anatomy and systematics of the sauropodomorph *Sarahsaurus aurifontanalis* from the Early Jurassic Kayenta Formation. *PLoS One*, **13**, e0204007.

Marsh, A. D. and Rowe, T. B. 2020. A comprehensive anatomical and phylogenetic evaluation of *Dilophosaurus wetherilli* (Dinosauria, Theropoda) with descriptions of new specimens from the Kayenta Formation of northern Arizona. *Journal of Paleontology*, **94, Suppl. S78**, 1–103.

Marsh, O. C. 1889. Notice of gigantic horned Dinosauria from the Cretaceous. *American Journal of Science*, **38**, 173–176.

Marsicano, C. A., Irmis, R. B., Mancuso, A. C., Mundil, R. and Chemale, F. 2016. The precise temporal calibration of dinosaur origins. *Proceedings of the National Academy of Sciences*, **113**, 509–513.

Martinez, R. N., Sereno, P. C., Alcober, O. A., Colombi, C. E., Renne, P. R., Montañez, I. P. and Currie, B. S. 2011. A basal dinosaur from the dawn of the dinosaur era in southwestern Pangaea. *Science*, **331**, 206–210.

Martz, J. and Parker, W. 2017. Revised formulation of the Late Triassic Land Vertebrate "Faunachrons" of western North America: recommendations for codifying nascent systems of vertebrate biochronology. 39–125. *In* Zeigler, K. E. and Parker, W. G. (eds) *Terrestrial depositional systems: Deciphering complexities through multiple stratigraphic methods*. Elsevier.

Mujal, E., Sues, H.-D., Moreno, R., Schaeffer, J., Sobral, G., Chakravorti, S., Spiekman, S. N. and Schoch, R. R. 2025. Triassic terrestrial tetrapod faunas of the Central European Basin, their stratigraphical distribution, and their palaeoenvironments. *Earth-Science Reviews*, **264**, 105085.

Müller, R. T., Langer, M. C., Bronzati, M., Pacheco, C. P., Cabreira, S. F. and Dias-Da-Silva, S. 2018. Early evolution of sauropodomorphs: anatomy and phylogenetic relationships of a remarkably well-preserved dinosaur from the Upper Triassic of southern Brazil. *Zoological Journal of the Linnean Society*, **184**, 1187–1248.

Nesbitt, S. J. and Chatterjee, S. 2008. Late Triassic dinosauriforms from the Post Quarry and surrounding areas, west Texas, USA. *Neues Jahrbuch für Geologie und Paläontologie-Abhandlungen*, **249**, 143–156.

Nesbitt, S. J. and Ezcurra, M. D. 2015. The early fossil record of dinosaurs in North America: a new neotheropod from the base of the Upper Triassic Dockum Group of Texas. *Acta Palaeontologica Polonica*, **60**, 513–526.

Nesbitt, S. J., Irmis, R. B. and Parker, W. G. 2007. A critical re-evaluation of the Late Triassic dinosaur taxa of North America. *Journal of Systematic Palaeontology*, **5**, 209–243.

Nesbitt, S. J., Smith, N. D., Irmis, R. B., Turner, A. H., Downs, A. and Norell, M. A. 2009. A complete skeleton of a Late Triassic saurischian and the early evolution of dinosaurs. *Science*, **326**, 1530–1533.

Nesbitt, S. J. and Sues, H.-D. 2021. The osteology of the early-diverging dinosaur *Daemonosaurus chauliodus* (Archosauria: Dinosauria) from the *Coelophysis* Quarry (Triassic: Rhaetian) of New Mexico and its relationships to other early dinosaurs. *Zoological Journal of the Linnean Society*, **191**, 150–179.

Niedźwiedzki, G., Brusatte, S. L., Sulej, T. and Butler, R. J. 2014. Basal dinosauriform and theropod dinosaurs from the mid–late Norian (Late Triassic) of Poland: implications for Triassic dinosaur evolution and distribution. *Palaeontology*, **57**, 1121–1142.

Novas, F. E., Agnolin, F. L., Ezcurra, M. D., Müller, R. T., Martinelli, A. G. and Langer, M. C. 2021. Review of the fossil record of early dinosaurs from South America, and its phylogenetic implications. *Journal of South American Earth Sciences*, **110**, 103341.

Novas, F. E., Ezcurra, M. D., Chatterjee, S. and Kutty, T. 2010. New dinosaur species from the Upper Triassic Upper Maleri and Lower Dharmaram formations of central India. *Earth and Environmental Science Transactions of the Royal Society of Edinburgh*, **101**, 333–349.

Olsen, P., Sha, J., Fang, Y., Chang, C., Whiteside, J. H., Kinney, S., Sues, H.-D., Kent, D., Schaller, M. and Vajda, V. 2022. Arctic ice and the ecological rise of the dinosaurs. *Science Advances*, **8**, eabo6342.

Owen, R. 1842. Report on British fossil reptiles. *Report of the British Association for the Advancement of Science*, **1842**, 60–204. https://www.biodiversitylibrary.org/page/33377524

Pacheco, C., Müller, R. T., Langer, M., Pretto, F. A., Kerber, L. and Da Silva, S. D. 2019. *Gnathovorax cabreirai*: a new early dinosaur and the origin and initial radiation of predatory dinosaurs. *PeerJ*, **7**, e7963.

Padian, K. 1989. Presence of the dinosaur *Scelidosaurus* indicates Jurassic age for the Kayenta Formation (Glen Canyon Group, northern Arizona). *Geology*, **17**, 438–441.

Raath, M. A. 1978. The anatomy of the Triassic theropod *Syntarsus rhodesiensis* (Saurischia: Podokesauridae) and a consideration of its biology. PhD dissertation. Rhodes University, 358 pp.

Ramezani, J., Hoke, G. D., Fastovsky, D. E., Bowring, S. A., Therrien, F., Dworkin, S. I., Atchley, S. C. and Nordt, L. C. 2011. High-precision U-Pb zircon geochronology of the Late Triassic Chinle Formation, Petrified Forest National Park (Arizona, USA): temporal constraints on the early evolution of dinosaurs. *Geological Society of America Bulletin*, **123**, 2142–2159.

Reig, O. A. 1963. La presencia de dinosaurios saurisquios en los "Estratos de Ischigualasto" (Mesotriasico Superior) de las provincias de San Juan y La Rioja (Argentina). *Ameghiniana*, **3**, 3–20.

Rinehart, L. F., Lucas, S. G., Heckert, A. B., Spielmann, J. A. and Celeskey, M. D. 2009. *The Paleobiology of Coelophysis bauri* (Cope) from the Upper Triassic (Apachean) Whitaker quarry, New Mexico, with detailed analysis of a single quarry block. New Mexico Museum of Natural History and Science, Bulletin 45.

Rogers, R. R., Swisher Iii, C. C., Sereno, P. C., Monetta, A. M., Forster, C. A. and Martínez, R. N. 1993. The Ischigualasto tetrapod assemblage (Late Triassic, Argentina) and 40Ar/39Ar dating of dinosaur origins. *Science*, **260**, 794–797.

Rowe, T. 1989. A new species of the theropod dinosaur *Syntarsus* from the Early Jurassic Kayenta Formation of Arizona. *Journal of Vertebrate Paleontology*, **9**, 125–136.

Rowe, T. B., Sues, H.-D. and Reisz, R. R. 2011. Dispersal and diversity in the earliest North American sauropodomorph dinosaurs, with a description of a new taxon. *Proceedings of the Royal Society B*, **278**, 1044–1053.

Sarıgül, V. 2017. New theropod fossils from the Upper Triassic Dockum Group of Texas, USA, and a brief overview of the Dockum theropod diversity. *PaleoBios*, **34**, 1–18.

Schwartz, H. L. and Gillette, D. D. 1994. Geology and taphonomy of the *Coelophysis* quarry, upper Triassic Chinle Formation, Ghost Ranch, New Mexico. *Journal of Paleontology*, **68**, 1118–1130.

Seeley, H. 1888. Classification of the Dinosauria. *Geological Magazine*, **5**, 45–46.

Sereno, P. C. 1997. The origin and evolution of dinosaurs. *Annual Review of Earth and Planetary Sciences*, **25**, 435–489.

Sereno, P. C., Forster, C. A., Rogers, R. R. and Monetta, A. M. 1993. Primitive dinosaur skeleton from Argentina and the early evolution of Dinosauria. *Nature*, **361**, 64–66.

Sereno, P. C. and Novas, F. E. 1994. The skull and neck of the basal theropod *Herrerasaurus ischigualastensis*. *Journal of Vertebrate Paleontology*, **13**, 451–476.

Smith-Paredes, D., Núñez-León, D., Soto-Acuña, S., O'Connor, J., Botelho, J. F. and Vargas, A. O. 2018. Dinosaur ossification centres in embryonic birds uncover developmental evolution of the skull. *Nature Ecology & Evolution*, **2**, 1966–1973.

Sömmerring, S. 1812. Über einen *Ornithocephalus*: Denkschriften der Königlich Bayerischen Akademie der Wissenschaften. *Mathematisch-Physikalische Klasse*, **3**, 89–158.

Srivastava, S. and Nesbitt, S. J. 2025. Project: A new taxon of saurischian dinosaur from the *Coelophysis* Quarry of New Mexico, USA (Triassic: latest Norian or Rhaetian) highlights herrerasaurian diversity in the latest Triassic [dataset]. MorphoSource. https://www.morphosource.org/projects/000794729

Stebbins, G. L. 1974. *Flowering plants: Evolution above the species level*. Harvard University Press.

Stocker, M. R. 2013. Conceptualizing vertebrate faunal dynamics: new perspectives from the Triassic and Eocene of Western North America. PhD dissertation. The University of Texas at Austin, 297 pp. http://hdl.handle.net/2152/22086

Sues, H.-D., Nesbitt, S. J., Berman, D. S. and Henrici, A. C. 2011. A late-surviving basal theropod dinosaur from the latest Triassic of North America. *Proceedings of the Royal Society B*, **278**, 3459–3464.

Vasconcelos, T., O'Meara, B. C. and Beaulieu, J. M. 2022. Retiring "cradles" and "museums" of biodiversity. *The American Naturalist*, **199**, 194–205.

Weeks, O. J., Cooper, R. B., Whiteside, D. I., Duffin, C. J., Copp, C., Hildebrandt, C., Hutchinson, D. and Benton, M. J. 2025. Microvertebrates from a Rhaetian neptunian dyke at Holwell, Somerset: dating the fissures. *Proceedings of the Geologists' Association*, **136**, 101112.

Welles, S. 1954. New Jurassic dinosaur from the Kayenta formation of Arizona. *Geological Society of America Bulletin*, **65**, 591–598.

Whiteside, J. H., Lindström, S., Irmis, R. B., Glasspool, I. J., Schaller, M. F., Dunlavey, M., Nesbitt, S. J., Smith, N. D. and Turner, A. H. 2015. Extreme ecosystem instability suppressed tropical dinosaur dominance for 30 million years. *Proceedings of the National Academy of Sciences*, **112**, 7909–7913.

Wilson, J. A. 2006. Anatomical nomenclature of fossil vertebrates: standardized terms or 'lingua franca'? *Journal of Vertebrate Paleontology*, **26**, 511–518.

Zeigler, K. E. and Geissman, J. W. 2011. Magnetostratigraphy of the Upper Triassic Chinle Group of New Mexico: implications for regional and global correlations among Upper Triassic sequences. *Geosphere*, **7**, 802–829.

Zeigler, K. E., Kelley, S. and Geissman, J. W. 2008. Revisions to stratigraphic nomenclature of the Upper Triassic Chinle Group in New Mexico: new insights from geologic mapping, sedimentology, and magnetostratigraphic/paleomagnetic data. *Rocky Mountain Geology*, **43**, 121–141.